Behavioral/Systems/Cognitive

Nicotinic Acetylcholine Receptors in the Mesolimbic Pathway: Primary Role of Ventral Tegmental Area $\alpha6\beta2^*$ Receptors in Mediating Systemic Nicotine Effects on Dopamine Release, Locomotion, and Reinforcement

Cecilia Gotti,[1]* Stefania Guiducci,[2]* Vincenzo Tedesco,[4] Silvia Corbioli,[5] Lara Zanetti,[2] Milena Moretti,[1] Alessio Zanardi,[2] Roberto Rimondini,[7] Manolo Mugnaini,[6] Francesco Clementi,[1] Christian Chiamulera,[4] and Michele Zoli[2,3]

[1]Consiglio Nazionale delle Ricerche, Institute of Neuroscience, Cellular and Molecular Pharmacology Center, Department of Medical Pharmacology, University of Milan, 20129 Milan, Italy, [2]Department of Biomedical Sciences, Section of Physiology, University of Modena and Reggio Emilia, and [3]Centro AntiFumo (Interdipartimentale), Azienda Ospedaliero–Universitaria Policlinico di Modena, 41100 Modena, Italy, [4]Neuropsychopharmacology Laboratory, Section of Pharmacology, Department of Medicine and Public Health, University of Verona, 37134 Verona, Italy, [5]Preclinical Drug Discovery and Enabling Technologies and [6]Addiction and Sleep Disorders Discovery Performance Unit, Neurosciences Center of Excellence for Drug Discovery, GlaxoSmithKline Medicines Research Center, 37135 Verona, Italy, and [7]Department of Pharmacology, University of Bologna, 40126 Bologna, Italy

$\alpha6^*$ nicotinic acetylcholine receptors (nAChRs) are highly and selectively expressed by mesostriatal dopamine (DA) neurons. These neurons are thought to mediate several behavioral effects of nicotine, including locomotion, habit learning, and reinforcement. Yet the functional role of $\alpha6^*$ nAChRs in midbrain DA neurons is mostly unknown. The aim of this study was to determine the composition and *in vivo* functional role of $\alpha6^*$ nAChR in mesolimbic DA neurons of male rats. Immunoprecipitation and immunopurification techniques coupled with cell-specific lesions showed that the composition of $\alpha6^*$ nAChR in the mesostriatal system is heterogeneous, with (non-$\alpha4$)$\alpha6\beta2^*$ being predominant in the mesolimbic pathway and $\alpha4\alpha6\beta2^*$ in the nigrostriatal pathway. We verified whether $\alpha6^*$ receptors mediate the systemic effects of nicotine on the mesolimbic DA pathway by perfusing the selective antagonists α-conotoxin MII (CntxMII) ($\alpha3/\alpha6\beta2^*$ selective) or α-conotoxin PIA (CntxPIA) ($\alpha6\beta2^*$ selective) into ventral tegmental area (VTA). The intra-VTA perfusion of CntxMII or CntxPIA markedly decreased systemic nicotine-elicited DA release in the nucleus accumbens and habituated locomotion; the intra-VTA perfusion of CntxMII also decreased the rate of nicotine infusion in the maintenance phase of nicotine, but not of food, self-administration. Overall, the results of these experiments show that the $\alpha6\beta2^*$ nAChRs expressed in the VTA are necessary for the effects of systemic nicotine on DA neuron activity and DA-dependent behaviors such as locomotion and reinforcement, and suggest that $\alpha6\beta2^*$-selective compounds capable of crossing the blood–brain barrier may affect the addictive properties of nicotine and therefore be useful in the treatment of tobacco dependence.

Introduction

The mesostriatal dopamine (DA) pathway is a major brain target of nicotine. Its ventral [the mesolimbic DA pathway, comprising cell bodies in the ventral tegmental area (VTA) and terminals in the nucleus accumbens (nAc) and tuberculum olfactorium] and dorsal [the nigrostriatal DA pathway, comprising cell bodies in the substantia nigra and terminals in the caudate–putamen (CPu)] components both express high levels of nicotinic acetylcholine receptors (nAChRs). These receptors are thought to mediate several main behavioral effects of nicotine, including the regulation of locomotor activity and reinforcement in the mesolimbic component and habit learning in the nigrostriatal component (Di Chiara, 2000; Janhunen and Ahtee, 2007).

Neuronal nAChRs comprise a heterogeneous family of pentameric oligomers made up of combinations of subunits encoded by at least 11 different genes in mammals. They have been grouped into two subfamilies based on their phylogenetic, functional, and pharmacological properties (Le Novère and Changeux, 1995; Corringer et al., 2000; Gotti et al., 2006), namely the α-bungarotoxin (Bgtx)-sensitive nAChRs ($\alpha7$, $\alpha9$, and $\alpha10$ subunits) and the Bgtx-insensitive nAChRs ($\alpha2$–$\alpha6$ and $\beta2$–$\beta4$ sub-

Received Oct. 13, 2009; revised March 2, 2010; accepted March 8, 2010.

This work was supported by Italian Project of Main National Interest (PRIN) Grant 20072BTSR2 (F.C., M.Z.); European Community Grant Neurocypres (C.G., M.Z.); a grant from the Neurosciences Center of Excellence for Drug Discovery, GlaxoSmithKline (Verona, Italy) (M.Z.); Fondazione Cariplo Grant 2006/0882/104878 and a grant from Associazione Oasi Maria Santissima (Troina, Italy) (F.C.); and Fondazione Cariplo Grant 2006/0779/109251 and Compagnia San Paolo Grant 2005-1964 (C.G.). We thank the technical assistance of Dr. Claudia Tregnago, Marzia Di Chio, Dr. Chiara Giuliano, Dr. Alessia Auber, Dr. Luca Zangrandi, Alberto Ruffo, and Federica Vinco. We thank Dr. Stefano Fontana and Dr. Mario Corsi for careful reading of this manuscript.

The authors declare no competing financial interests.

*C.G. and S.G. contributed equally to this work.

Correspondence should be addressed to Michele Zoli, Department of Biomedical Sciences, Section of Physiology, University of Modena and Reggio Emilia, via Campi 287, 41100 Modena, Italy. E-mail: michele.zoli@unimore.it.

DOI:10.1523/JNEUROSCI.5095-09.2010

 0270-6474/10/305311-15$15.00/0

units). These latter subunits can combine to form a number of functionally and pharmacologically different heteropentamers consisting of two to four different subunits.

Most nAChR subunits are expressed in midbrain DA neurons (Le Novère et al., 1996; Charpantier et al., 1998; Azam et al., 2002). Two main populations of Bgtx-insensitive nAChRs are expressed by DA cell body/dendrite compartment of the ventral midbrain, α4(non-α6)β2* and α6β2* nAChRs (Klink et al., 2001; Champtiaux et al., 2003). However, their complete subunit composition and possible cellular or subcellular heterogeneity are not known. Much more is known on the composition of nAChRs expressed by striatal DA terminals. Converging immunochemical and neurochemical evidence (Grady et al., 2007) demonstrate the presence of four main populations: α4β2, α4α5β2, α6β2(β3), and α4α6β2(β3) nAChRs. Less is known on their regional and cellular heterogeneity. Yet a recent paper showed that α6β2 responses dominate in the nAc but not in the CPu (Exley et al., 2008).

Much evidence has been collected on the functions of α6β2* nAChRs in *in vitro* and *ex vivo* preparations (Champtiaux et al., 2003; Salminen et al., 2004; Grady et al., 2007; Drenan et al., 2008). In addition, some recent papers have started to elucidate the functional role of α6* nAChRs *in vivo*, showing their involvement in nicotine-elicited locomotion (Drenan et al., 2008) and nicotine self-administration (Pons et al., 2008; Brunzell et al., 2010).

The purpose of the present experiments is to assess the role of α6β2* nAChRs of the mesolimbic DA pathway in mediating *in vivo* neurochemical and behavioral effects of systemic nicotine. With this aim, we identified nAChR composition in these neurons, dissecting the different components of the mesostriatal system, in particular distinguishing the nigrostriatal from the mesolimbic DA pathway, and examined the effects of the selective α6β2* nAChR antagonists α-conotoxin MII (CntxMII) and α-conotoxin PIA (CntxPIA) (Dowell et al., 2003) administered into the VTA or the nAc through microdialysis cannulae, on main neurochemical and behavioral effects of systemic nicotine.

Materials and Methods

Animals and materials

Adult male pathogen-free Sprague Dawley rats (Charles River) were used. All animal experimentation was conducted in accordance with the European Communities Council Directive of 24 November 1986 (86/609/EEC).

(+/−)[^{3}H]Epibatidine (Epi) [specific activity (s.a.), 50–66 Ci/mmol] and [*N*-methyl-^{3}H]nisoxetine (s.a., 82 Ci/mmol) were purchased from GE Healthcare, ^{125}I-Epi (s.a., 2200 Ci/mmol) and ^{3}H-labeled (−)-2-β-carbomethoxy-3-β-(4-fluorophenyl)tropane ([^{3}H]WIN 35,428) (s.a., 86 Ci/mmol) were from PerkinElmer, and nonradioactive ligands were from Sigma-Aldrich. CntxMII, α-conotoxin MII [H9A,L15A] (CntxMIImod) (McIntosh et al., 2004), and CntxPIA were custom synthesized by NeoMPS. Complete Mini, a specific mixture of peptidase inhibitors, was obtained from Roche Diagnostic. Aprotinin, leupeptin, pepstatin, and phenylmethylsulfonyl fluoride (PMSF) were purchased from Sigma-Aldrich.

In self-administration experiments, nicotine hydrogen tartrate (Sigma-Aldrich) was dissolved in heparinized bacteriostatic saline (0.9% NaCl plus 0.9% benzyl alcohol plus 1 IU/ml heparin), and pH was adjusted to 7.4 with NaOH. Nicotine unit doses are expressed as milligrams of free base/kilogram of body weight/infusion.

Immunoprecipitation and immunopurification experiments

Antibody production and characterization. The polyclonal antibodies against the α2, α3, α4, α5, α6, β2, β3, and β4 nAChR subunits were produced in rabbit as previously described (Gotti et al., 2005a,b) and affinity purified. The peptides obtained from mouse, rat, or human sequences were located in the putative cytoplasmic (CYT) loop between M3 and M4 and/or at the C terminal. For almost all of the subunits, we raised antisera directed against two separate peptides of the same subunit and the immunoprecipitation values reported are the mean of results obtained using both antisera. For a full characterization of nAChR-subunit antibodies, see Grady et al. (2009), their supplemental Table 1. The affinity-purified antisera were bound to CNBr-activated Sepharose at a concentration of 1 mg/ml, and the columns used for subtype immunopurification.

Characterization of antibody specificity was performed using nAChR subunit knock-out mice, brain region extracts and cells transfected with subunit cDNAs as described previously (Zoli et al., 2002; Champtiaux et al., 2003; Moretti et al., 2004; Gotti et al., 2005a).

6-Hydroxydopamine and N*-2-chlorethyl-*N*-ethyl-2-bromobenzylamine lesions and eye enucleation.* Unilateral denervation of mesostriatal DA pathways was performed by injecting the selective neurotoxin 6-hydroxydopamine (6OHDA) (10 μg/4 μl) in the medial forebrain bundle [coordinates from bregma: anterior (A), −4 mm; lateral (L), 1.8 mm; deep (D), −7.5 mm] (Paxinos and Watson, 2007). [^{3}H]WIN 35,428 binding was determined individually in dorsal and ventral striata and ventral midbrain from unlesioned and 6OHDA-lesioned rats using a saturating concentration of 100 nM [^{3}H]WIN 35,428 in the presence or absence of 10 μM GBR 12935 [1-(2-(diphenylmethoxy)ethyl)-4-(3-phenylpropyl)piperazine]. 6OHDA-lesioned tissues with a decrease of [^{3}H]WIN 35,428 <80% were discarded.

Noradrenaline (NA) denervation was obtained by injection of the selective toxin *N*-2-chlorethyl-*N*-ethyl-2-bromobenzylamine (DSP-4) (50 mg/kg, i.p.; Sigma-Aldrich). The animals were killed 14 d after the toxin injection, and the dorsal and ventral striatum as well as ventral midbrain were dissected and rapidly frozen. Binding of [*N*-methyl-^{3}H]nisoxetine, a selective ligand for noradrenaline transporter, was used to assess the extent of NA terminal degeneration.

Bilateral enucleation of the eyes was performed to examine the effects of retinal deafferentation on nAChR subtype expression in mesostriatal regions. Enucleation was performed under deep anesthesia with halothane (Merial Italia). The extraocular muscles were cut until reaching the optic nerve. The optic nerve was exposed and cut, and the eye was completely removed. The remaining cavity was filled with Gelfoam embedded in xylocaine and sealed with cyanoacrylamide gel. The enucleated rats were killed 14 d after the enucleation to allow for degeneration of retinogeniculate and retinocollicular pathways (Lund et al., 1976).

Brain region dissection. Selected regions were manually dissected from fresh brain coronal sections. Dorsal and ventral striatum were dissected from coronal sections that span from bregma level 0 to +2.5 mm. Dorsal striatum comprised the CPu, whereas ventral striatum comprised nAc, rostral ventral pallidum, and tuberculum olfactorium. Ventral midbrain was dissected from coronal sections that span from bregma level −4.8 to −6.0 mm, taking away the interpeduncular nucleus.

Preparation of membranes and 2% Triton X-100 extracts. The tissues were immediately frozen in liquid nitrogen and stored at −80°C for later use. In every experiment, the tissues (0.2 g) were homogenized in 10 ml of 50 mM sodium phosphate, pH 7.4, 1 M NaCl, 2 mM EDTA, 2 mM EGTA, and 2 mM PMSF with a Potter homogenizer. The homogenates were then diluted and centrifuged for 1.5 h at 60,000 × *g*. The procedures of homogenization, dilution, and centrifugation of the total membranes were performed twice, after which the pellets were collected, rapidly rinsed with 50 mM Tris-HCl, pH 7, 120 mM NaCl, 5 mM KCl, 1 mM $MgCl_2$, 2.5 mM $CaCl_2$, and 2 mM PMSF, and then resuspended in the same buffer containing a mixture of 20 μg/ml of each of the following protease inhibitors: leupeptin, bestatin, pepstatin A, and aprotinin. Triton X-100 at a final concentration of 2% was added to the washed membranes, which were extracted for 2 h at 4°C. The extracts were then centrifuged for 1.5 h at 60,000 × *g* and recovered, and an aliquot of the resultant supernatants was collected for protein measurement using the BCA protein assay (Pierce) with bovine serum albumin as the standard.

[N-methyl-^{3}H]Nisoxetine binding. The binding of nisoxetine to membranes, obtained from control and treated animals, was performed as previously described (Cheetham et al., 1996) with minor modifications.

Briefly, tissues were homogenized using a Potter in ice-cold 50 mM Tris-HCl, pH 7.4, containing 120 mM NaCl and 5 mM KCl, diluted, and centrifuged as described by Cheetham et al. (1996). Saturation binding experiments were performed using final [*N*-methyl-^{3}H]nisoxetine concentrations ranging from 0.1 to 15 nM at 4°C for 4 h. Nonspecific binding (averaging 10–20% of total binding) was determined in parallel by means of incubation in the presence of 1 μM unlabeled nisoxetine (Sigma-Aldrich). At the end of the incubation, the samples were filtered on a GFC filter soaked in 0.5% polyethylenimine and washed with 15 ml of 10 mM sodium phosphate, pH 7.4, plus 50 mM NaCl, and the filters were counted in a beta counter.

^{125}I-α-bungarotoxin binding. Binding experiments were performed by incubating striatal or midbrain membranes overnight with 2–4 nM ^{125}I-Bgtx (specific activity, 200 Ci/mmol) (PerkinElmer) at 20°C in the presence of 2 mg/ml BSA. Specific radioligand binding was defined as total binding minus nonspecific binding determined in the presence of 1 μM cold Bgtx (Sigma-Aldrich).

Immunoprecipitation of [^{3}H]epibatidine-labeled receptors by anti-subunit-specific antibodies. Tissue extracts were preincubated with 2 μM Bgtx, labeled with 2 nM [^{3}H]Epi, and incubated overnight with a saturating concentration of affinity-purified anti-subunit IgG (20–30 μg) (Sigma-Aldrich). The immunoprecipitation was recovered by incubating the samples with beads containing bound anti-rabbit goat IgG (Technogenetics). The level of antibody immunoprecipitation was expressed as the percentage of [^{3}H]Epi-labeled receptors immunoprecipitated by the antibodies (taking the amount present in the Triton X-100 extract solution before immunoprecipitation as 100%) or as femtomoles of immunoprecipitated receptors/milligram of protein.

Receptor subtype immunopurification. For each purification experiment, the dorsal and ventral striatum from 20 to 30 animals was dissected and immediately frozen at −80°C and processed as described by Gotti et al. (2005a). The extract was incubated three times with 5 ml of Sepharose 4B-bound anti-α6 antisera (anti-α6 CYT) to remove the α6* receptors. The α6-depleted flow-through fraction was collected for additional processing. The bound α6* population was eluted from column by means of incubation with 100 μM α6 CYT peptide. The flow-through and the eluted receptors were analyzed by immunoprecipitation using subunit-specific antibodies, as described above, after labeling with 2 nM [^{3}H]Epi.

Deduction of receptor subtype composition. To obtain a quantitative evaluation of the subunit composition of a receptor subtype, it is necessary to evaluate the efficiency of immunoprecipitation of antigens by their respective antisera. For our subunit-specific antisera, we found an efficiency of immunoprecipitation ranging from 75 to 90%. This suggests that the figures that we obtained in this study are probably slightly underestimated. In addition, in defining nAChR subtypes in striatum and ventral midbrain, we followed the current hypothesis that heteromeric nAChRs comprise two subunits bearing the principal amino acid loops for acetylcholine binding interfaces (i.e., α2, α3, α4, or α6 subunits) and two subunits bearing the complementary amino acid loops for acetylcholine binding interfaces (i.e., β2 or β4 subunits), whereas the fifth subunit can be either a complementary subunit, or a principal subunit (α3 or α4 subunits), or a purely structural subunit (α5 or β3 subunits) (Gotti et al., 2009).

Pharmacological experiments on immunoimmobilized native subtypes

The affinity-purified anti-α3, α6, β2, or β4 antibodies were bound to microwells (Maxi-Sorp; Nunc) by means of overnight incubation at 4°C at a concentration of 10 μg/ml in 50 mM phosphate buffer, pH 7.5. On the following day, the wells were washed to remove the excess of unbound antibodies and then incubated overnight at 4°C with 200 μl of 2% Triton X-100 superior colliculus, cerebral cortex, or cerebellum membrane extract containing 5–10 fmol of ^{125}I-Epi binding sites. After incubation, the wells were washed, and the presence of immobilized receptors revealed by means of ^{125}I-Epi binding.

For saturation experiments, ^{125}I-Epi was used at concentration ranging from 0.005 to 0.5 nM. For inhibition experiments, the immunoimmobilized receptors were incubated [30 min, room temperature (RT)] with various concentrations of toxins before adding ^{125}I-Epi at the K_d concentration. Incubation was prolonged overnight at 4°C. Nonspecific binding was measured in the presence of 100 nM unlabeled Epi.

Pharmacological experiments on HEK cells transfected with human α3β2 subtype

HEK cells transiently transfected with α3β2 human subunits were a generous gift from Prof. Fabrizio Eusebi (Università La Sapienza, Rome, Italy). Binding to membrane was performed overnight by incubating aliquots of the cell membrane with [^{3}H]Epi concentrations ranging from 0.005 to 2 nM at 4°C. Nonspecific binding (averaging 5–10% of total binding) was determined in parallel by means of incubation in the presence of 100–250 nM unlabeled Epi.

For inhibition experiments, the immunoimmobilized receptors were incubated (30 min; RT) with various concentrations of toxins before adding [^{3}H]Epi at the K_d concentration. At the end of the incubation, the samples were centrifuged and washed once with 10 sodium phosphate, pH 7.4, plus 50 mM NaCl, the pellet was dissolved with 2N NaOH, and the filters were counted in a beta counter.

α-Conotoxin MII free fraction in plasma and brain tissue

Equilibrium dialysis: evaluation of plasma and brain tissue binding. Plasma and brain unbound fractions were determined in a 96-well equilibrium dialysis apparatus (HTDialysis) using a previously reported method (Kalvass and Maurer, 2002). In brief, fresh rat plasma and brain tissue were obtained the day of the study. Membranes (12–14 kDa cutoff), obtained from Spectrum Laboratories, were conditioned in HPLC water for 60 min, followed by 20% ethanol for 20 min, and 100 mM sodium phosphate, pH 7.4, buffer for 15 min.

Brain tissue was diluted twofold with a surrogate buffer for CSF (7.3 g/L NaCl, 186.4 mg/L KCl, 239.9 mg/L $MgCl_2$, 185.2 mg/L $CaCl_2$, and 536.0 mg/L $Na_2HPO_4{\cdot}7H_2O$, pH 7.4), and it was subjected to homogenization using an Autogizer (Tomtec).

CntxMII was added to samples of plasma and brain tissue homogenate (10 μg/ml and 10 μg/g, respectively), and 150 μl aliquots ($n = 6$) were loaded into the 96-well equilibrium dialysis apparatus and dialyzed against an equal volume of 100 mM sodium phosphate, pH 7.4, buffer for plasma or against surrogate CSF (see above) for brain tissue homogenates. Equilibrium was achieved by incubating the 96-well equilibrium dialysis apparatus in a temperature-controlled incubator at 37°C (Elettrofor Scientific Instrument) for 5 h, using an orbital shaker at 125 rpm (Elettrofor Scientific Instrument).

At the end of the incubation period, 50 μl aliquots of plasma or brain homogenate and buffers were transferred to a 96-deep-well plate, and the composition in each tube was balanced with control fluid, such that the volume of buffer to brain or plasma was the same. Sample extraction was performed by the addition of 400 μl of acetonitrile containing an internal standard. The samples were vortex-mixed and centrifuged, and the supernatant was analyzed by the HPLC–mass spectrometry (MS)/MS as described below.

Plasma unbound fraction was calculated from the ratio of analyte peak areas determined in buffer versus plasma samples. Equation 1, which accounts for the effect of tissue dilution on unbound fraction (Kalvass and Maurer, 2002), was used to calculate the brain unbound fraction as follows:

$$f_{\text{u-undiluted}} = \frac{(1/D)}{[(1/f_{\text{u-diluted}} - 1) + 1/D]}, \quad (1)$$

where D is dilution factor in brain homogenate, and $f_{\text{u-diluted}}$ is the measured free fraction of diluted brain tissue.

Samples analysis. All samples were analyzed by means of HPLC-MS/MS on a PerkinElmerSciex Instruments API-4000 tandem quadrupole mass spectrometer (Applied Biosystems), using a Turbo V Ionspray operated at a source temperature of 600°C (80 psi of nitrogen). The liquid chromatography/tandem MS was operated in positive-ion, multiple-reaction monitoring mode. The parent/daughter ion pair for CntxMII was 856.0 (double-charged ion)/109.9. Samples (10 μl) were injected using a CTC Analytics HTS Pal autosampler onto a Synergy RP MAX 4 μm, 2.0 × 30 mm column (Phenomenex) at an eluent flow rate of 1.5 ml/min. Analytes were eluted using a high-pressure linear gradient pro-

gram, by means of an HP1100 binary HPLC system (Agilent Technologies), using deionized H_2O containing 0.1% (v/v) formic acid as solvent A and acetonitrile containing 0.1% (v/v) formic acid as solvent B. The gradient was held at 5% solvent B for 0.3 min, before increasing to 95% at 1.0 min, remaining at 95% until 1.5 min before returning to the starting conditions. The cycle time was 1.9 min per sample, and typical run times ranged from 2.4 to 2.7 min.

Stability. Experiments to assess CntxMII recovery were designed to evaluate the stability of CntxMII in rat plasma and brain homogenate samples. CntxMII was added to samples of plasma and brain tissue homogenate (10 μg/ml and 10 μg/g, respectively), and 150 μl aliquots ($n = 3$) for each matrix were immediately processed as previously described at the end of the incubation period, whereas 150 μl aliquots ($n = 3$) for each matrix were incubated over for 5 h at 37°C (see above). At the end of the incubation period, 50 μl aliquots of plasma or brain homogenate were transferred to a 96-deep-well plate, and the composition in each tube was balanced with control fluid, such that the volume of buffer to brain or plasma was the same.

All samples were vortex-mixed and centrifuged, and the supernatants were analyzed by the HPLC-MS/MS as described above. For dialysis sample stability average analyte peak area was compared between solutions of incubated and fresh spiked matrix. This comparison was performed in presence and in absence of protease inhibitors.

Microdialysis procedure

Rats were anesthetized with halothane (see above) and placed in a flat skull position in a Kopf stereotaxic apparatus. A microdialysis probe (CMA/12; 2 mm dialysis membrane; 100,000 Da cutoff; CMA/Microdialysis) was inserted through a guide cannula into the right ventral striatum at the following coordinates from bregma: A, +1.7 mm; L, 0.8 mm; D, −6.0 mm from dura (Ferrari et al., 2002; Paxinos and Watson, 2007) (supplemental Fig. 1, available at www.jneurosci.org as supplemental material). In some experiments, in addition to the cannula in the nAc, a second cannula was inserted in the ipsilateral VTA at the following coordinates from bregma: A, −5.3 mm; L, 0.8 mm; and D, −6.2 mm from dura (Paxinos and Watson, 2007). The guide cannulae were permanently secured with dental cement. After surgery, the rats were placed in a circular Plexiglas cage and allowed to recover overnight before the microdialysis experiment. One or 2 d after insertion of the guide cannula, the microdialysis probe was inserted into the guide cannula The inlet tubing of the probe was connected to a microinjection pump (CMA/100; CMA/Microdialysis) and perfused with artificial CSF (aCSF) (2.5 mM KCl, 125 mM NaCl, 1.26 mM $CaCl_2$, 1.18 mM $MgCl_2$, 2 mM Na_2HPO_4, pH 7.4) at a flow rate of 1.1 μl/min (22 μl/20 min sample).

Detection of dopamine

A 20 μl volume from each sample was injected into an HPLC system with electrochemical detection for determination of DA concentration (ESA coulometric detector with a 5014 B cell; voltage: E1, −150 mV; E2, +220 mV) (Coulochem II Electrochemical Detector). Separation of DA was performed on an ESA HR-80 column (80 mm × 4.6 mm inner diameter). The mobile phase consisted of 18% methanol in 75 mM NaH_2PO_4, 1 mM 1-octanesulfonic acid (sodium octane sulfonate), and 20 μM EDTA, pH 5.6. The flow rate was 0.8 ml/min (Shimadzu LC-10AD_{VP}, Solvent Delivery Module). The chromatograms were integrated using Jasco Borwin HPLC software. DA detection limit was 5 fmol/sample.

Habituated locomotion

Animals were deeply anesthetized with halothane (see above), and two microdialysis probe guide cannulae (see above) were implanted into the right and left VTA (coordinates from bregma: A, −5.3 mm; L, 3.0 mm; D, −6.3 mm from dura; the cannulae were inserted with an angle of 16°) and secured to the skull with dental cement. One to 3 d after surgery, the awake animal was gently restrained by the experimenter and a microdialysis probe (see above) was inserted into each guide cannula. The probes were connected to a microinfusion pump (see above) and continuously perfused at 1.1 μl/min with aCSF.

Locomotor activity was measured in motility cages (Macrolon III; 38 × 20 × 16 cm) equipped with a lower row of four infrared beams for detection of horizontal movements and an upper row of four infrared beams for vertical movements (MED Associates). Interbeam distance was 8 cm horizontally and 6 cm vertically, and horizontal activity was recorded for 2 h in 5 min intervals (MED-PC Software). The animals were placed into the cages for a 60 min habituation period (Ferrari et al., 2002) and then perfused through the two dialysis cannulae with conotoxin or aCSF. Fifteen minutes after the start of conotoxin perfusion, the rats were injected with nicotine (0.4 mg/kg, base, i.p.) or vehicle. Habituated locomotion was measured for 60 min after the treatment.

Nicotine self-administration

Subjects. Rats were individually housed in a temperature-controlled environment (21–23°C) on a 12 h light/dark cycle (60 lx) with light on at 7:00 A.M. Animals were food restricted by 85–90% to maintain their body weight range between 240 and 260 g (daily checked): rats were fed *ad libitum* up to a body weight of ~290–300 g (average weight for 3 consecutive days), and then the 85% of their average body weight was calculated (~250 g), and their daily diet reduced and maintained stable (by daily checking body weight) for the rest of the study. Food diet (three to four pellets, for a total of 15–20 g/d) was made available after each experimental session. The maximum amount of sucrose pellet intake during training sessions was 4.5 g/d for those subjects meeting the criteria (see below, Training to lever press). Animals had *ad libitum* access to water except during experimental sessions.

Rats were trained or tested once daily. All animal procedures were performed in accordance with the Principles of Laboratory Animal Care (National Institutes of Health Publication No. 85-23, revised 1985), the European Communities Council Directive of 24 November 1986 (86/609/EEC). These procedures have been approved by the Interdepartmental Centre for Laboratory Animal Service and Research of the Università degli Studi di Verona, according to article 7 D.L. 116/92 of the Italian legislation. All efforts were made to minimize animal suffering and to keep the lowest number of animals used.

Apparatus. Behavioral testing was conducted in eight operant chambers (Coulbourn Instruments) encased in sound-insulated cubicles, equipped with ventilation fans (Ugo Basile). Each chamber was equipped with two levers, symmetrically centered on the front panel, and located 12.5 cm apart, 1 cm above the grid floor. The food magazine was situated in an opening in the panel between the two levers, 1 cm above the floor. This opening was closed during nicotine self-administration training. A 2 W white house light was located 26 cm above the food magazine and activated during the entire session duration, except during time-out (TO) periods. Right lever presses corresponding to fixed-ratio (FR) values required by the schedule of reinforcement produced the delivery of 45 mg sucrose pellet (Bioserv) or the activation of the infusion pump (model A-99Z; Razel Scientific Instruments). Nicotine solutions were administered via the infusion pump at a volume of 0.027 ml during a 1 s period. Sucrose pellet delivery was signaled by the 1 s illumination of a 4 W white stimulus light located in the same hole of the food magazine only during the training for lever press. During self-administration sessions, reinforcer delivery (nicotine infusion or sucrose pellet) was signaled by 1 s turn-on of one yellow and one green light-emitting diode centrally placed above the food magazine. Left lever presses ("inactive lever presses") did not have any consequence. All types of lever presses, sucrose pellet and infusion deliveries were recorded. Lever presses were also recorded during TO periods. Data acquisition and schedule parameters were controlled by a Med-PC software (MED Associates) running on a PC computer interfaced with the chambers via interface modules (MED Associates).

Training to lever press. After a 24 h food deprivation period, rats were trained to lever press for food as a reinforcer. The final training schedule of reinforcement was a FR2, session duration up to 60 min. Once subjects met the criteria of at least 25 reinforcers/1 h session (it required between 6 and 10 daily sessions), rats underwent surgery.

Surgery. Rats were anesthetized with 0.5 mg · kg^{-1} · 0.5 ml^{-1} medetomidine (Domitor; Pfizer), 10 mg/kg tiletamine plus 10 mg/kg zolazepam (Zoletil 100; Virbac; 0.2 ml/kg, i.m.), and then implanted with (1) a silicon catheter (inner diameter, 0.30 mm; outer diameter, 0.63 mm; Cam Caths) in the right jugular vein, and (2) two microdialysis guide

cannulae (see above) bilaterally into the right and left VTA (coordinates from bregma: A, −5.3 mm; L, 3.0 mm; D, −6.3 mm from dura; the cannulae were inserted with an angle of 16°) and secured to the skull with dental cement. Immediately after surgery, animals were medicated with 5 $mg \cdot kg^{-1} \cdot 1\ ml^{-1}$ subcutaneous carprophene (Rimadyl; Pfizer) and 25,000,000 IU of benzylpenicilline plus 1 g/kg dihydrostreptomycin (Rubrocillina Forte; Intervet; 1 ml/kg, s.c.), 0.5 $mg \cdot kg^{-1} \cdot 0.1\ ml^{-1}$ intramuscular atipamezole (Antisedan; Pfizer). Each day after recovery, animals received 0.1 ml of one intravenous injection of heparin solution (30 IU/ml heparin sodium; Sigma-Aldrich) before and after the experimental session to check catheter patency. In case of no in or out flushing, catheter patency was assessed by loss of righting reflex induced by pentobarbitone sodium (50 mg/kg) intravenous infusion through the catheter. Rats not responding to pentobarbitone were removed from the study.

Training in the nicotine self-administration procedure. This procedure has been described previously (Chiamulera et al., 2010). After the period of recovery, rats were trained to intravenously self-administer nicotine (FR1: nicotine, 0.03 $mg \cdot kg^{-1} \cdot infusion^{-1}$; TO, 60 s; session duration up to 25 infusions were delivered or 3 h elapsed, no priming injection). Adjustment of nicotine concentration to changes in rat body weight was not needed since rat body weight was kept stable at 250 g (±10 g). Lever pressing during the TO period was also recorded, although it did not have any consequence. If the animals met the criterion of 25 infusions within the end of the daily session, the FR value was increased to FR2 and then to FR3 with session duration lasting up to 1 h.

Rats were considered to reach a stable responding on nicotine self-administration under a FR3 schedule of reinforcement when the value of reinforcers/session did not vary >20% between three consecutive sessions.

CntxMII treatment. On test day, two microdialysis probes (see above) were inserted into the VTA guide cannulae. Then, rats were placed in a plastic bowl and external tips of the probes were connected to an inlet tubing coming from a microinfusion pump (see above) that delivered first aCSF for 30 min and, then, 10 μM CntxMII in aCSF, or aCSF alone (control) for 15 min, at a flow rate of 1.1 μl/min. Immediately after, rats were placed in Skinner box and underwent nicotine self-administration session with a schedule of reinforcement, FR3: 0.03 $mg \cdot kg^{-1} \cdot infusion^{-1}$ nicotine; TO, 60 s; 1 h session.

Each rat received both treatments (CntxMII or aCSF) in a balanced order on different daily sessions (test sessions) with at least three daily sessions elapsing (baseline sessions) to assess stability of responding.

Food-maintained responding

Rats allocated to food-maintained responding test were initially trained to lever press for food (similarly to rats undergoing nicotine self-administration experiments) (see above, Training for lever press) and then exposed to a slightly different FR2 schedule for food reinforcement: FR2, TO, 60 s period; session duration, up to 60 min. At stable performance of responding for food reinforcement (values did not vary >20% between three consecutive sessions), FR value was increased to FR3.

Stable responding for food on FR3 schedule was reached after 11.7 ± 4.8 sessions (mean ± SD). At stability, the average number of food reinforcers/session was 54.8 ± 0.8. Rate of responding was 346.6 ± 52.1 active lever presses and 4.5 ± 1.9 inactive lever presses (means ± SEM of the last three food-responding sessions before starting the testing phase; data only from rats with correct VTA guide cannulae placements; $n = 6$).

Determination of probe location in in vivo *procedures*

At the end of microdialysis, locomotion, or self-administration experiments, the animal was killed with a lethal injection of pentobarbital (65 mg/kg, i.p.), its brain was removed from the skull, and the position of the microdialysis probes was verified by visual inspection of the fresh tissue or the frozen brain during cut at the cryostat. The probe track was visible as a small hemorrhagic line. Data from brains with large hemorrhages (>2 mm in diameter) or misplaced probe(s) location were discarded. In an average experiment with 15 animals (control plus treatment), we had one to two rats discarded because of a large hemorrhage and two rats discarded because of probe misplacement (supplemental Fig. 1, available at www.jneurosci.org as supplemental material).

Statistical analysis

The experimental data obtained from the saturation binding experiments performed on immunoimmobilized $\alpha6\beta2^*$, $\alpha4\beta2^*$, or $\alpha3\beta4^*$ subtypes or membrane-bound $\alpha3\beta2$ subtype were analyzed by means of a nonlinear least-square procedure using the LIGAND program as described by Munson and Rodbard (1980). The calculated binding parameters were obtained by simultaneously fitting three independent experiments. The selection of the best fitting (i.e., one-site versus two-site model) and evaluation of the statistical significance of the parameters (i.e., comparison of the binding parameters of the two groups) were based on the F test for the "extra sum of square" principle. A value of $p < 0.05$ was considered statistically significant (Munson and Rodbard, 1980). The K_i values of the toxins on Epi binding were determined by means of the LIGAND program using the data obtained from three independent experiments and compared by means of the F test as described above.

DA perfusate levels after nicotine administration were expressed as percentage of the last three basal values. Differences in treatment groups were then analyzed by repeated-measures ANOVA (time as within factor and treatment as between factor) (statistical package, SPSS, version 12). When a significant treatment effect was observed, the data were further analyzed with Bonferroni's or Dunnett's test for multiple comparisons. Number of beam breaks in habituated locomotion experiments was analyzed with the same statistical approach.

Since each rat received both treatments, the effects of CntxMII or aCSF pretreatment on nicotine self-administration and food-maintained responding were assessed by paired sample Student's t test comparing differences (test session − respective baseline session) in the CntxMII and aCSF tests for each rat (statistical package, SPSS, version 12).

For all analyses, $p < 0.05$ was considered to be the threshold for statistical significance.

Results

nAChR composition in dorsal and ventral striatum, and ventral midbrain

In a previous paper (Zoli et al., 2002), we determined nAChR subunit composition of DA and non-DA neurons in homogenates of total striatum. Our aim here is to distinguish nAChRs of the nigrostriatal [dorsal striatum (i.e., CPu)] and mesolimbic [ventral striatum (i.e., mainly nAc and tuberculum olfactorium)] pathways.

nAChR subunits expressed in DA neurons of dorsal and ventral striatum

We first determined the overall composition of nAChRs expressed by different neuronal populations by studying [^{3}H]Epi-labeled receptor immunoprecipitation by subunit-specific antisera. We studied control, intact, animals, animals lesioned with the DA neuron-selective toxin 6OHDA, and animals with bilateral eye enucleation. 6OHDA caused an almost complete loss of DA cell structures as shown by a >90% decrease in [^{3}H]WIN 35,428 binding (data not shown). Since the retina is a major source of nAChR subtypes with uncommon neuronal subunits (such as $\alpha2$, $\alpha3$, $\alpha5$, $\alpha6$, and $\beta3$) (Moretti et al., 2004; Gotti et al., 2005b; Cox et al., 2008), we performed bilateral eye enucleation to assess a possible contribution of these minor subtypes from visual afferents. A third major source of $\alpha6^*$ nAChRs in the brain is the locus ceruleus, where high levels of $\alpha6$ mRNA have been detected (Le Novère et al., 1996). However, in preliminary experiments, we showed that lesion of the noradrenergic pathway with the selective toxin DSP-4 does not alter [^{3}H]Epi binding in the dorsal or ventral striatum, or ventral midbrain (supplemental Fig. 2, available at www.jneurosci.org as supplemental material).

Although the concentration of [^{3}H]Epi-labeled receptors was much higher in dorsal (172 ± 11 fmol/mg protein) (data not shown) than in ventral striatum (94 ± 8 fmol/mg protein) (data not shown), the overall nAChR subunit composition was remarkably similar in the two regions (Fig. 1*A*,*B*). Bilateral eye

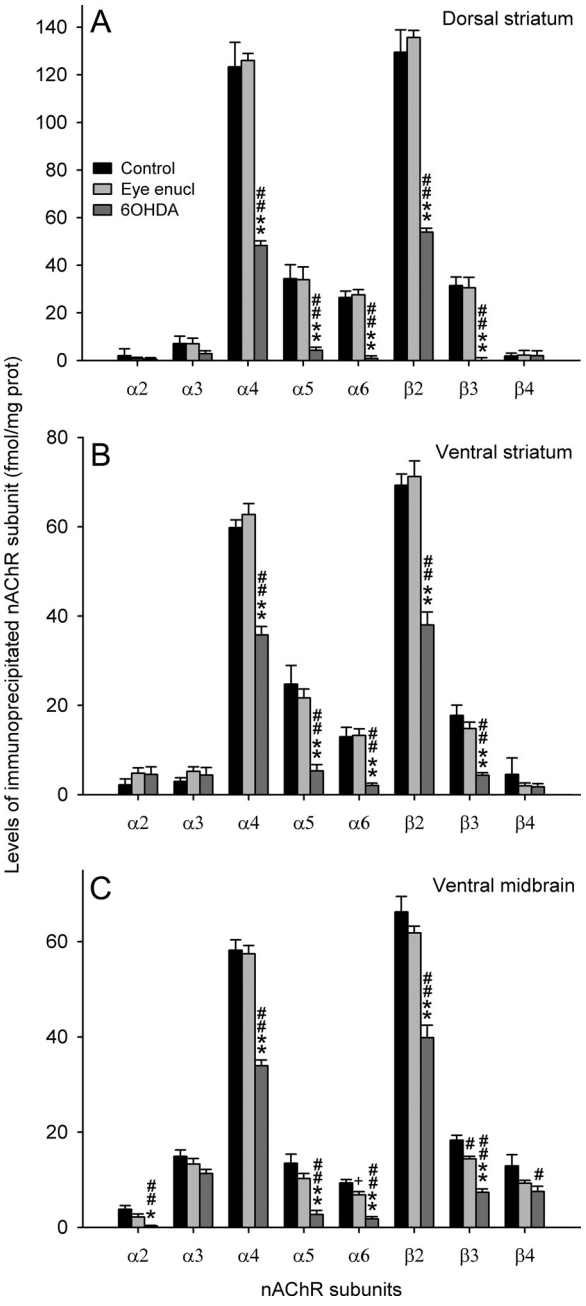

Figure 1. ***A–C***, Immunoprecipitation of nAChR subunits in 2% Triton X-100 extracts of dorsal striatum (***A***), ventral striatum (***B***), or ventral midbrain (***C***) from control rats and rats that underwent bilateral eye enucleation or bilateral injection of 6OHDA into the medial forebrain bundle. Each value represents the mean ± SEM of five to nine separate determinations performed in triplicate. Statistical analysis was according to one-way ANOVA followed by Bonferroni's test. $^{**}p < 0.01$, $^{*}p < 0.05$ versus eye enucleation; $^{\#\#}p < 0.01$, $^{\#}p < 0.05$, $^{+}0.10 < p > 0.05$ versus control (ctrl). ***A***, α2: $F_{(2,16)} = 0.29$, NS; α3: $F_{(2,16)} = 1.10$, NS; α4: $F_{(2,16)} = 70.46$, $p < 0.001$; 6OHDA versus eye, $p < 0.001$; 6OHDA versus control, $p < 0.001$; α5: $F_{(2,16)} = 8.43$, $p = 0.003$; 6OHDA versus eye, $p = 0.010$; 6OHDA versus ctrl, $p = 0.006$; α6: $F_{(2,16)} = 18.47$, $p < 0.001$; 6OHDA versus eye, $p < 0.001$; 6OHDA versus ctrl, $p < 0.001$; β2: $F_{(2,16)} = 8.69$, $p = 0.003$; 6OHDA versus eye, $p = 0.008$; 6OHDA versus ctrl, $p = 0.006$; β3: $F_{(2,16)} = 14.37$, $p < 0.001$; 6OHDA versus eye, $p < 0.001$; 6OHDA versus ctrl, $p < 0.001$; β4: $F_{(2,16)} = 0.01$, NS. ***B***, α2: $F_{(2,17)} = 0.99$, NS; α3: $F_{(2,17)} = 0.87$, NS; α4: $F_{(2,17)} = 57.47$, $p < 0.001$; 6OHDA versus eye, $p < 0.001$; 6OHDA versus ctrl, $p < 0.001$; α5: $F_{(2,17)} = 18.05$, $p < 0.001$; 6OHDA versus eye, $p < 0.001$; 6OHDA versus ctrl, $p < 0.001$; α6: $F_{(2,17)} = 22.03$, $p < 0.001$; 6OHDA versus eye, $p < 0.001$; 6OHDA versus ctrl, $p < 0.001$; β2: $F_{(2,17)} = 42.27$, $p < 0.001$; 6OHDA versus eye, $p < 0.001$; 6OHDA versus ctrl, $p < 0.001$; β3: $F_{(2,17)} = 22.08$, $p < 0.001$; 6OHDA versus eye, $p < 0.001$; 6OHDA versus ctrl, $p < 0.001$; β4: $F_{(2,17)} = 0.75$, NS. ***C***, α2: $F_{(2,20)} = 9.84$, $p = 0.001$; eye versus ctrl, NS; 6OHDA versus eye, $p = 0.037$; 6OHDA versus ctrl, $p = 0.001$; α3: $F_{(2,19)} = 2.20$, NS; α4: $F_{(2,16)} = 49.94$, $p < 0.001$; eye versus ctrl, NS; 6OHDA versus eye, $p < 0.001$; 6OHDA versus ctrl, $p < 0.001$; α5: $F_{(2,15)} = 15.03$, $p < 0.001$; eye versus ctrl, NS; 6OHDA versus eye, $p = 0.003$; 6OHDA versus ctrl, $p < 0.001$; α6: $F_{(2,15)} = 24.97$, $p < 0.001$; eye versus ctrl, $p = 0.069$; 6OHDA versus eye, $p < 0.001$; 6OHDA versus ctrl, $p < 0.001$; β2: $F_{(2,15)} = 32.81$, $p < 0.001$; eye versus ctrl, NS; 6OHDA versus eye, $p < 0.001$; 6OHDA versus ctrl, $p < 0.001$; β3: $F_{(2,12)} = 39.49$, $p < 0.001$; eye versus ctrl, $p = 0.013$; 6OHDA versus eye, $p < 0.001$; 6OHDA versus ctrl, $p < 0.001$; β4: $F_{(2,18)} = 3.87$, $p = 0.040$; eye versus ctrl, NS; 6OHDA versus eye, NS; 6OHDA versus ctrl, $p = 0.037$.

Table 1. Composition of nAChR subtypes expressed by DA neurons of dorsal and ventral striatum and ventral midbrain as deduced from immunoprecipitation experiments

	% of total β2* nAChRs (% of α6* nAChRs)		
nAChR subtype	Dorsal striatum	Ventral striatum	Ventral midbrain
α4β2	20.5	11.3	29.8
α2α4β2	0	0	8.0
α4α5β2	39.5	53.4	32.2
α4β2β3	6.4	1.1	8.6
α4α6β2β3	29.9 (89.0)	13.7 (40.0)	21.4 (100.0)
α6β2β3	3.7 (11.0)	20.5 (60.0)	0 (0)
α4*	96.3	79.5	100.0
α4 (non-α6)*	66.4	65.8	78.6
α6*	33.6	34.2	21.4

enucleation did not significantly alter nAChR subunit concentration in the two regions. 6OHDA significantly decreased α4 and β2 subunit levels and caused an almost complete loss of α5, α6, and β3 subunits in both regions. Although the same pattern of subunit decrease was observed in the two regions, the deduced subtype composition in DA neurons showed some interesting heterogeneity between dorsal and ventral striatum (Table 1) (for rules and caveats to be used in deductions about nAChR composition starting from immunoprecipitation experiments, see Materials and Methods). In dorsal striatum, ~90% of the overall α6* nAChR population also contained α4 subunit, presumably forming a receptor with an α6β2 binding interface and an α4β2 binding interface, whereas in the ventral striatum only 40% of the overall α6* nAChR population contained α4 subunit. Therefore, in the ventral striatum, ~60% of α6* nAChRs have two α6β2 binding interfaces.

Previous immunopurification experiments in extracts of total striatum (Zoli et al., 2002) showed that α5 subunit is associated with α4* nAChRs, whereas β3 subunit is associated with α6* nAChRs. This picture is coherent with present data as regards ventral striatum, where the concentration of [^{3}H]Epi receptors immunoprecipitated by α6 and β3 subunit antibodies is very similar (α6, 11.1 fmol/mg protein; β3, 11.5 fmol/mg protein). However, in the dorsal striatum, the amount of β3* nAChRs is larger than that of α6* nAChRs (α6, 26.4 fmol/mg protein; β3, 31.4 fmol/mg protein) (Fig. 1*A*). Therefore, we hypothesize the presence of a minor population (~6% of total nAChRs) of α4β3β2 receptors selectively present in DA terminals of the CPu (Table 1).

We also studied ^{125}I-Bgtx binding (a marker of α7* nAChRs) in dorsal and ventral striatum and ventral midbrain, and found no significant difference between 6OHDA or eye-enucleated rats and control rats in any region examined (supplemental Fig. 3, available at www.jneurosci.org as supplemental material).

α6 and non-α6* nAChRs expressed in dorsal and ventral striatum*

To confirm this subtype heterogeneity, we performed immunopurification experiments using an affinity column bearing

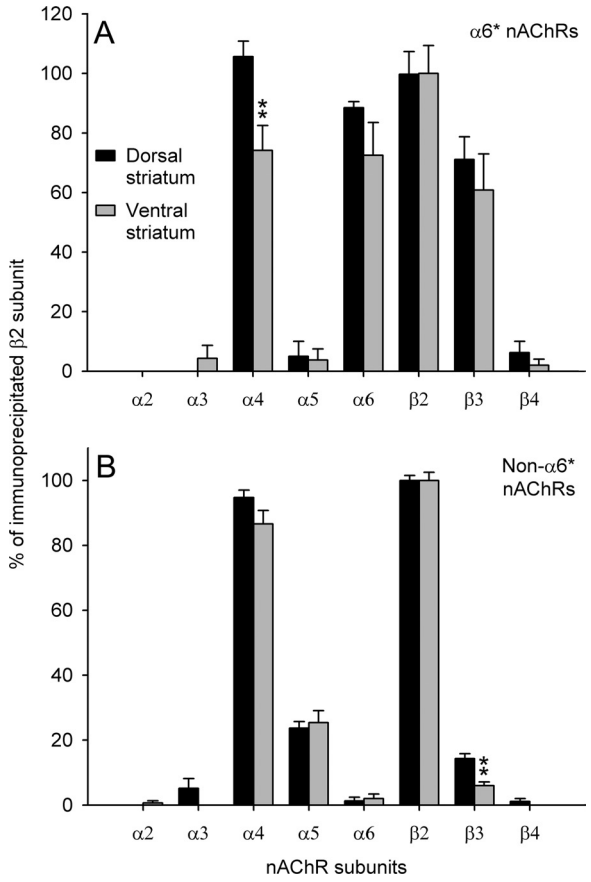

Figure 2. ***A***, ***B***, Immunoprecipitation analysis of the subunit content of α6* (***A***) and non-α6* (***B***) nAChR subtypes immunopurified through affinity column from striatal extracts and labeled with 2 nM [^{3}H]Epi. The results are expressed as percentage of total [^{3}H]Epi binding immunoprecipitated by β2 antibody. Each data point is the mean ± SEM of three to five determinations performed in triplicate. Statistical analysis was according to independent-sample Student's *t* test; $^{**}p < 0.01$. ***A***, α4: df = 10, $t = 3.21$, $p = 0.009$. ***B***, β3: df = 16, $t = 4.51$, $p < 0.001$.

anti-α6 antibody. Although quantitation with this method is less accurate because of the addition of additional steps in the procedure than quantitation obtained with immunoprecipitation, immunopurification experiments give a direct demonstration of the presence of a subunit in a receptor population. Selective α6* nAChR immunodepletion was confirmed by the fact that immunoprecipitated α6-containing [^{3}H]Epi-labeled receptors decreased from 15.4 ± 1.5 and 12.9 ± 2.4% to 1.3 ± 1.1 and 2.0 ± 1.4% in the flow-through of the α6 column from dorsal and ventral striatal extract, respectively. As shown in Figure 2*A*, in the dorsal striatum all receptors immunopurified on the α6 column (α6* nAChRs) had α4 subunit, whereas in the ventral striatum <75% of α6* receptors contained an α4 subunit. This significant difference in the content of α4 subunit in α6* immunopurified receptors tallies well with the findings of immunoprecipitation experiments and confirms the existence of a substantial population of α6(non-α4)* nAChRs in the ventral, but not dorsal, striatum.

As regards the analysis of the flow-through from α6 columns, the only significant difference between dorsal and ventral striatum was a higher content of β3 subunit in the dorsal striatum (Fig. 2*B*). Also, these results tally well with the immunoprecipitation findings and confirm the existence of a minor population of α4(non-α6)β3β2 nAChRs in the dorsal striatum that is marginally, or not, represented in the ventral striatum.

nAChR subunits expressed in DA neurons of ventral midbrain

We made an attempt to determine what nAChR subtypes are expressed in DA cell bodies and dendrites of the ventral midbrain. Because of the relatively little amount of nAChRs that can be recovered from this region, we sampled homogenates of the entire ventral midbrain (without interpeduncular nucleus) (see Materials and Methods) and could not distinguish between the neurons of origin of the nigrostriatal pathway (substantia nigra) and those of the mesolimbic pathway (VTA).

A significant decrease and a trend for a significant decrease, respectively, were detected in the levels of β3 and α6 nAChR subunits in rats that underwent bilateral eye enucleation (Fig. 1*C*). This finding tallies well with the evidence of very high levels of CntxMII binding in the medial terminal nucleus of the accessory optic tract (MT) (Mugnaini et al., 2006). 6OHDA-induced DA neuron degeneration markedly decreased α4, β2, and β3 subunit levels and caused an almost complete loss of α2, α5, and α6 subunits (Fig. 1*C*). This pattern differs from what has been observed in DA terminals of both dorsal and ventral striatum as regards α2 and β3 subunits (see above). In fact, α2 decrease in 6OHDA-treated rats was observed only in the ventral midbrain. Indeed, differently from striatal levels, DA denervation caused only a partial loss of β3 subunit in the ventral midbrain implying that in this region there exists a substantial population of β3* nAChRs not expressed by DA neurons. Very likely, non-DAergic β3 subunit is associated with α3β4* nAChRs expressed in the fasciculus retroflexus that crosses the ventral midbrain, as recently shown in immunoprecipitation experiments (Grady et al., 2009).

The composition of nAChR subtypes expressed by DA neurons in the ventral midbrain deduced from present immunoprecipitation experiment is reported in Table 1.

nAChR subtype selectivity of conotoxins

Immunoprecipitation and immunopurification studies described above confirm and further refine the notion that α6β2* nAChRs constitute a major receptor population expressed by both cell body/dendrite compartment and nerve terminal compartment of the nigrostriatal and mesolimbic DA pathways. To characterize the contribution of these receptors to the neurochemical and behavioral effects of systemic nicotine, we decided to use α6β2*-selective antagonists, namely CntxMII, CntxMIImod (an analog of CntxMII that was reported to have higher selectivity for α6β2* receptors) (McIntosh et al., 2004), and CntxPIA, in the awake freely moving animals. We first determined the affinity of these toxins for α6β2* and other nAChR subtypes expressed in the rat ventral midbrain and striatum.

α6β2 nAChRs immunopurified from rat superior colliculus membranes*

Saturation binding analysis revealed an affinity for ^{125}I-Epi binding of 38 pM (Table 2). CntxMII competition binding studies were performed, and, in agreement with previously reported data (Champtiaux et al., 2003; Gotti et al., 2005b), we found that the α6β2* nAChRs have a statistically significant better fit for a two site model with high [K_i of 3 nM; coefficient of variation (CV), 39%] and low affinity ($K_i > 10$ μM; CV, 41%) for CntxMII (Fig. 3, Table 2). The high- and low-affinity sites are thought to correspond to binding at α6β2 and α4β2 interfaces, respectively (Zoli et al., 2002; Champtiaux et al., 2003; Gotti et al., 2005a). The CntxMIImod showed a single site presumably for the α6β2 subtype with relatively low affinity (K_i of 1.8 μM; CV, 57%). The CntxPIA also showed a statistically significant better fit for a two-

Table 2. Binding of conotoxins to purified nAChR subtypes

	K_d for ^{125}I-epibatidine	K_i (CV) for α-conotoxin MII	K_i (CV) for α-conotoxin MII [H9A,L15A]	K_i (CV) for α-conotoxin PIA
α6β2* purified from superior colliculus	38 pM	3 nM (39%) and >10 μM	1.8 μM (57%)	37 nM (59%)
α3β2* purified from HEK cells	35 pM	55 nM (59%)[a]	>10 μM	>10 μM
α4β2* purified from cerebral cortex	33 pM	>10 μM	>10 μM	>10 μM
α3β4* purified from cerebellum	98 pM	>10 μM	>10 μM	>10 μM

[a]The K_i value of CntxMII was found to be 115 nM for α3β2* nAChRs immunopurified from rat superior colliculus (Gotti et al., 2005b).

site model with high- (K_i of 37 nM; CV, 59%) and low-affinity ($K_i > 10$ μM) sites.

α3β2 nAChRs immunopurified from rat superior colliculus and HEK cells*

Immunoimmobilized α3β2* nAChRs from superior colliculus proved to have a too low concentration to be used in competition experiments. Therefore, the analysis of α3β2* nAChRs was performed on receptors purified from HEK cells transfected with human α3 and β2 subunit. Saturation binding analysis revealed an affinity for ^{125}I-Epi binding of 35 pM (Table 2). When tested on the membrane-bound α3β2 receptors, the CntxMII showed an affinity of 55 nM (CV, 37%), which is similar to the value of 115 nM previously detected with immunopurified α3β2* nAChRs from rat superior colliculus (Gotti et al., 2005b). Both the CntxMIImod and CntxPIA showed a very low affinity for this subtype with K_i values of >10 and 11 μM, respectively (Fig. 3).

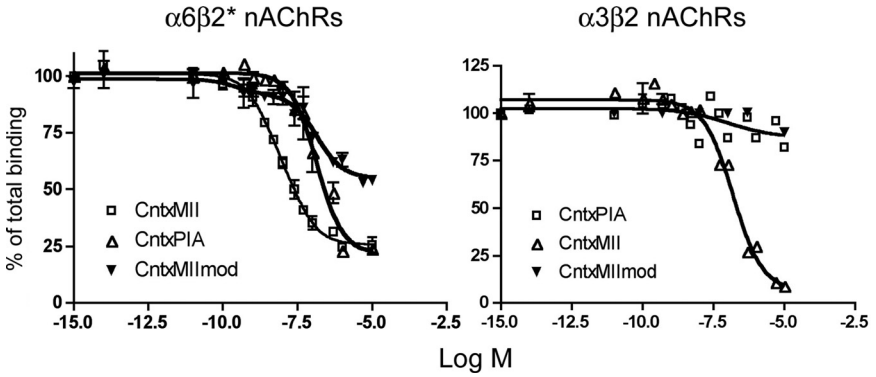

Figure 3. Inhibition of ^{125}I-Epi binding to immunoimmobilized α6β2* and α3β2* nAChRs by CntxMII [H9A, L15A] (CntxMIImod), and CntxPIA. The curves were obtained by fitting three to four separate experiments using the LIGAND program. Error bars indicate SEM.

α4β2 and α3β4* nAChRs immunopurified from rat cerebral cortex and cerebellum, respectively*

Saturation binding analysis revealed an affinity for ^{125}I-Epi binding of 33 and 98 pM for α4β2* and α3β4* receptors, respectively. All three toxins showed a very low affinity (>10 μM) toward the α4β2* or α3β4* subtypes (Table 2).

On the basis of these results, we confirmed that CntxMII has high affinity for both α6β2* and α3β2* subtypes, whereas CntxPIA only has high affinity for the α6β2* subtype. Instead, our batch of CntxMIImod did not show high affinity for native α6β2 interface and was not used in the following experiments.

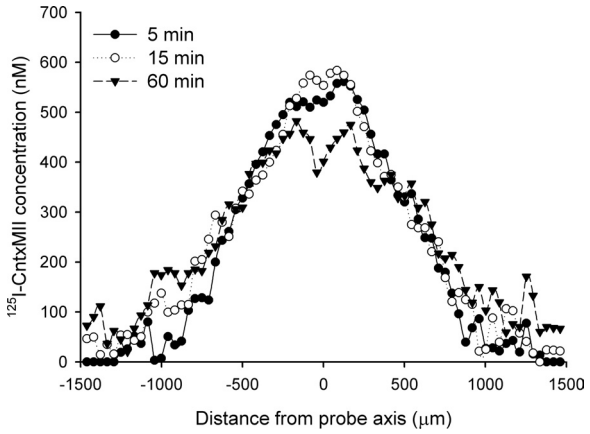

Figure 4. Intra-VTA diffusion of ^{125}I-CntxMII perfused through a microdialysis cannula. The figure shows the levels of ^{125}I-CntxMII concentration at different distances from the probe after 5, 15, or 60 min perfusion of 10 μM ^{125}I-CntxMII. The values are the mean of three experiments.

Setup of the method for the intracerebral perfusion of conotoxins

Since conotoxins, being peptidic molecules, cannot cross the blood–brain barrier (Blanchfield et al., 2007), we thought to administer them intracerebrally via perfusion through a microdialysis cannula. In a set of preliminary experiments, we studied CntxMII availability in brain tissue after perfusion through a microdialysis cannula with a large (100,000 Da) cutoff. With this aim, we determined the diffusion of ^{125}I-CntxMII from a microdialysis cannula into the brain (Fig. 4), the free (unbound) concentration of CntxMII in brain tissue (Table 3), and the biological efficacy of CntxMII locally perfused at the concentration of 10 μM (supplemental Fig. 4, available at www.jneurosci.org as supplemental material).

To assess the intracerebral diffusion of CntxMII after perfusion of the toxin through a microdialysis cannula, we perfused ^{125}I-CntxMII (2000 Ci/mmol, 10 μM dissolved in aCSF) through a microdialysis probe (100,000 Da cutoff) located in the VTA, followed by killing of the animal after 5, 15, or 60 min of perfusion and autoradiographical detection of the labeled toxin. The results are shown in Figure 4. The central part of the labeled area corresponds to the trace of the cannula and has a high concentration of radioactivity, corresponding to 500–600 nM ^{125}I-CntxMII. This is ~5% of the concentration of CntxMII present in the solution perfused through the cannula. Decrease of labeled toxin from the site of probe location follows an exponential decay. The concentration of radioactive CntxMII at 1 mm far from the cannula drops to 18, 82, and 105 nM after 5, 15, and 60 min of perfusion, respectively.

Brain tissue binding experiments, using equilibrium dialysis methodology, showed that only a limited (<10%) fraction of CntxMII in a brain homogenate is unbound and therefore available for binding to target receptors (Table 3) (for additional details, see supplemental material, available at www.jneurosci.org as supplemental material).

From these experiments, we can derive that a reasonable estimate of the effective concentration of CntxMII perfused into the brain from a dialysis probe varies between 0.5 and 0.1% of the

Table 3. Conotoxin MII rat plasma protein and brain tissue binding determined at 10 μg/ml and 10 μg/g, respectively, after 5 h incubation on a 96-well equilibrium dialysis plate (HTDialysis)

Matrix (Lister hooded rats)	fu%	
	Brain	Plasma
Values	7.09	49.61
	5.92	57.35
	9.13	56.96
	9.71	55.45
	7.79	49.83
	7.57	47.58
Mean	7.87	>50
SD	1.38	NM
Median	7.68	>50
Range	[5.92–9.71]	[47.58 to >50]

Abbreviations: fu, Fraction unbound; NM, not measurable.

perfused concentration within a distance of 1 mm far from the dialysis membrane.

Effects of intra-nAc or intra-VTA perfusion of conotoxins on systemic nicotine-elicited DA release in the nAc

Effects of intra-nAc or intra-VTA perfusion of CntxMII

We first tested the effects of CntxMII perfusion into the nAc or the VTA on DA perfusate levels from the nAc. With this aim, we performed double-probe microdialysis experiments (Zanetti et al., 2007), placing a probe in the shell subregion of the nAc for DA detection and another probe in the anterior VTA. To test the effects of intra-nAc CntxMII administration, CntxMII was perfused through the microdialysis cannula in the nAc, whereas aCSF was infused into the VTA. To test the effects of intra-VTA administration of CntxMII, CntxMII was perfused through the intra-VTA probe, whereas aCSF was perfused into the nAc. The dose of CntxMII (10 μM) was selected on the basis of preliminary experiments (see above). In both intra-nAc and intra-VTA experiments, CntxMII was perfused 15 min before a systemic administration of nicotine (0.4 mg/kg, i.p., nicotine base) (Ferrari et al., 2002).

Peripheral nicotine injection was able to significantly increase by ~55% DA perfusate levels in the medial nAc ($n = 7$ rats). Although local perfusion of CntxMII in the nAc did not cause a significant change in nicotine-elicited increase in DA levels ($n = 6$ rats), local perfusion in the VTA completely abolished DA increase in the nAc ($n = 5$ rats) (repeated-measures ANOVA, time: $F_{(1,15)} = 64.43, p < 0.001$; groups: $F_{(2,15)} = 5.7, p = 0.014$; time by groups: $F_{(2,15)} = 9.63$, $p = 0.002$; *post hoc* Dunnett's test: Nic+CntxMII-VTA vs Nic+aCSF, $p = 0.008$; Nic+CntxMII-nAc vs Nic+aCSF, NS) (Fig. 5).

Lack of effect of intra-nAc perfusion of CntxMII was confirmed in an independent experiment using 1 or 10 μM doses (Fig. 6). CntxMII (1 or 10 μM) or aCSF were perfused into the nAc through a microdialysis probe starting 15 min before systemic nicotine (0.4 mg/kg, i.p., nicotine base) administration. No significant difference between CntxMII (1 μM) ($n = 4$), CntxMII (10 μM) ($n = 5$), and aCSF ($n = 10$) perfusion was detected (repeated-measures ANOVA, time: $F_{(5,16)} = 5.42, p < 0.001$; groups: $F_{(2,16)} = 0.03, p = 0.997$; time by groups: $F_{(10,16)} = 1.50, p = 0.154$) (Fig. 6).

We, therefore, focused our subsequent analysis on nAChRs expressed in the VTA. This is in accordance with a previous paper (Nisell et al., 1994) showing that intra-VTA but not intra-nAc infusion of the nonselective antagonist mecamylamine decreased nicotine-elicited DA release in nAc. We do not, however, exclude that additional analysis of CntxMII-sensitive nAChRs of the nAc using different experimental paradigms would evidence their

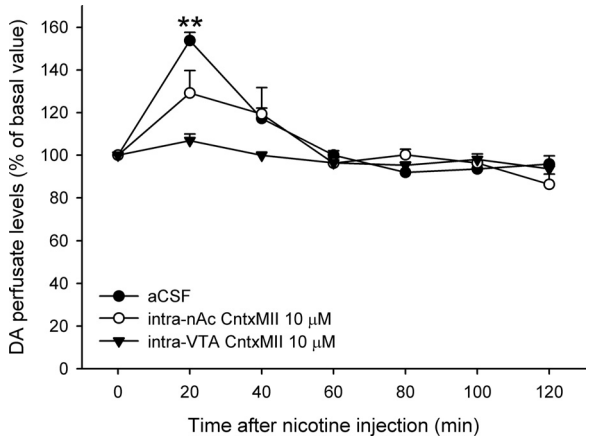

Figure 5. Effects of intra-nAc or intra-VTA perfusion of 10 μM CntxMII (15 min before nicotine administration) on perfusate DA levels in nAc elicited by nicotine (0.4 mg/kg base, i.p.). Mean ± SEM values are expressed as percentage of the last three baseline values before nicotine injection. Statistical analysis was according to repeated-measures ANOVA; $^{**}p < 0.01$ versus Nic+aCSF. Group size: aCSF, seven rats; CntxMII-nAc, six rats; CntxMII-VTA, five rats.

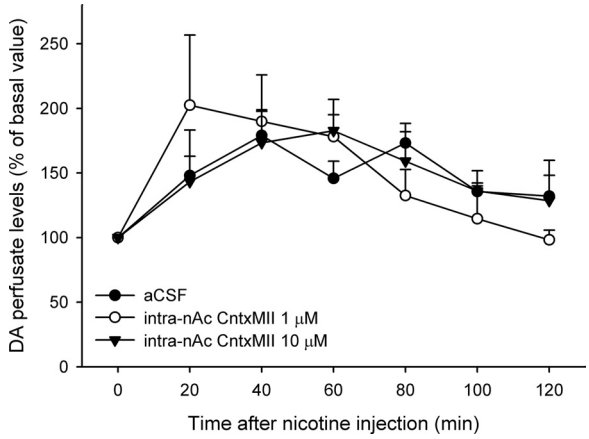

Figure 6. Effects of intra-nAc perfusion of CntxMII (1 or 10 μM) on DA dialysate levels from the nAc. Mean ± SEM values are expressed as percentage of the last three baseline values before nicotine injection. Statistical analysis was according to repeated-measures ANOVA. No significant group effect was detected. Group size: aCSF, 10 rats; CntxMII (1 μM), 4 rats; CntxMII (10 μM), 5 rats.

contribution to the effects of systemic nicotine on DA release in nAc, as suggested by several lines of evidence obtained in *ex vivo* preparations (Grady et al., 2007; Exley et al., 2008). It is possible that, with the present experimental approach, nAChRs expressed by nAc DA terminals outside of the access region of the CntxMII diffusing from the microdialysis cannula were not inhibited, so that DA continued to be released by the systemic nicotine. This released DA might reach the microdialysis probe, such that the intra-nAc CntxMII would appear to be ineffective. Indeed, our data on local perfusion of CntxMII plus nicotine (supplemental Fig. 4, available at www.jneurosci.org as supplemental material) indicate that CntxMII-sensitive receptors of the nAc can be activated by nicotine also *in vivo*. Finally, a very recent paper showed that infusion of CntxMII into the nAc shell was able to decrease nicotine self-administration (Brunzell et al., 2010).

Effects of intra-VTA perfusion of CntxMII: dose–response study

We then decided to explore in more detail the intra-VTA effects of CntxMII. The effects on systemic nicotine-elicited release of DA by three more doses of CntxMII (1 μM, 100 nM, and 10 nM)

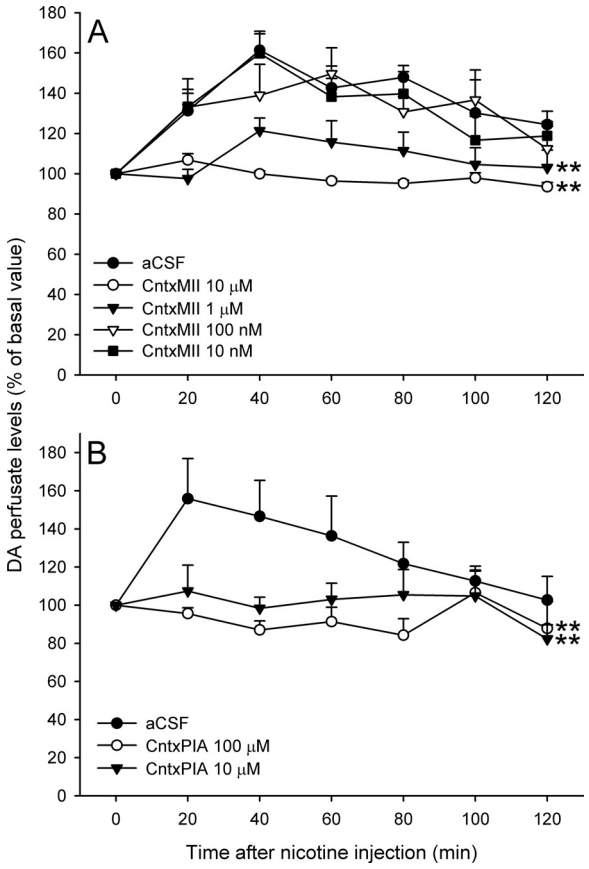

Figure 7. ***A***, ***B***, Effects of intra-VTA perfusion (15 min before nicotine administration) of different concentrations of CntxMII (***A***) or CntxPIA (***B***) on perfusate DA levels in nAc elicited by nicotine (0.4 mg/kg base, i.p.). Mean ± SEM values are expressed as percentage of the last three baseline values before nicotine injection. Statistical analysis was according to repeated-measures ANOVA. ***A***, $^{**}p < 0.01$ versus aCSF. Group size: aCSF, six rats; CntxMII (10 nM), six rats; CntxMII (100 nM), eight rats; CntxMII (1 μM), eight rats; CntxMII (10 μM), five rats. ***B***, $^{**}p < 0.01$ versus aCSF. Group size: aCSF, four rats; CntxPIA (10 μM), five rats; Cntx-PIA (100 μM), nine rats.

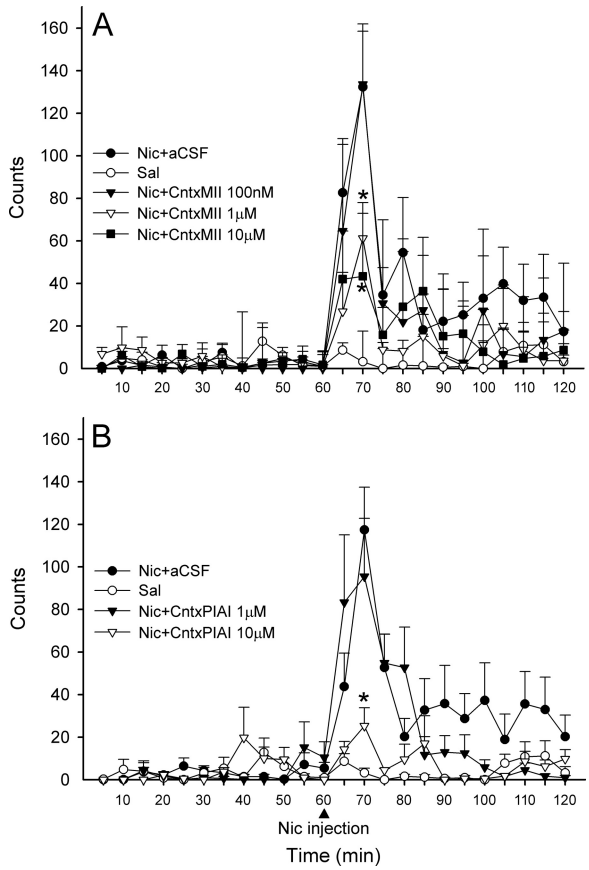

Figure 8. ***A***, ***B***, Effects of intra-VTA perfusion (15 min before nicotine administration) of different concentrations of CntxMII (***A***) or CntxPIA (***B***) on habituated locomotion elicited by nicotine (0.4 mg/kg base, i.p.). Mean values are shown. Error bars indicate SEM. Statistical analysis was according to repeated-measures ANOVA. ***A***, $^{*}p < 0.05$ versus Nic+aCSF. Group size: Saline, five rats; aCSF, six rats; CntxMII (100 nM), five rats; CntxMII (1 μM), five rats; CntxMII (10 μM), six rats. ***B***, $^{*}p < 0.05$ versus Nic+aCSF. Group size: Saline, five rats; aCSF, seven rats; CntxPIA (1 μM), six rats; CntxPIA (10 μM), four rats.

perfused into the VTA were tested in the double-probe microdialysis paradigm described above. Whereas 100 and 10 nM CntxMII did not significantly differ from aCSF, DA perfusate levels in the nAc in rats perfused with 1 μM CntxMII into the VTA significantly differed from vehicle as well as from 100 or 10 nM CntxMII-perfused rats [repeated-measures ANOVA, time: $F_{(5,24)} = 6.57$, $p < 0.001$; groups: $F_{(3,24)} = 6.23$, $p = 0.003$; time by groups: $F_{(15,24)} = 0.79$, NS; *post hoc* Dunnett's test vs Nic+aCSF: Nic+CntxMII (1 μM), $p = 0.003$; Nic+CntxMII (100 nM), NS; Nic+CntxMII (10 nM), NS] (Fig. 7*A*).

Effects of intra-VTA perfusion of CntxPIA

To confirm CntxMII effects and refine the subtype selectivity of the effect, we tested two doses of CntxPIA (100 and 10 μM) in the double-probe paradigm. As shown above, this toxin has lower affinity than CntxMII for α6β2* nAChRs but higher selectivity with respect to α3β2* nAChRs (Table 2). Both CntxPIA doses blocked nicotine-elicited increase in DA perfusate levels in the nAc (Fig. 7*B*), indicating that the effect is attributable to blockade of α6β2 receptors in the VTA [repeated-measures ANOVA, time: $F_{(5,15)} = 2.57$, $p = 0.033$; groups: $F_{(2,15)} = 13.88$, $p < 0.001$; time by groups: $F_{(10,15)} = 1.47$, NS; *post hoc* Dunnett's test vs Nic+aCSF: Nic+CntxPIA (10 μM), $p = 0.004$; Nic+CntxPIA (100 μM), $p < 0.001$].

Effects of intra-VTA perfusion of conotoxins on systemic nicotine-elicited habituated locomotion

Effects of CntxMII and CntxPIA perfused into the VTA

In this paradigm, conotoxins were perfused into the VTA through bilateral microdialysis cannulae. At both 10 and 1 μM doses, CntxMII perfused starting 15 min before nicotine injection was able to markedly decrease the increased locomotor activity elicited by an intraperitoneal injection of nicotine (0.4 mg/kg, base, i.p.), whereas CntxMII 100 nM was ineffective [repeated-measures one-way ANOVA, $F_{(4,22)} = 8.75$, $p < 0.001$; Dunnett's *post hoc* test vs Nic+aCSF: Nic+CntxMII (100 nM), NS; Nic+CntxMII (1 μM), $p = 0.015$; Nic+CntxMII (10 μM), $p = 0.013$] (Fig. 8*A*). At 10 μM dose, CntxPIA was able to markedly decrease nicotine stimulation of locomotion, whereas CntxPIA at 1 μM was ineffective [repeated-measures one-way ANOVA, $F_{(3,18)} = 6.95$, $p = 0.003$; Dunnett's *post hoc* test vs Nic+aCSF: Nic+CntxPIA (1 μM), NS; Nic+CntxPIA (10 μM), $p = 0.044$] (Fig. 8*B*).

As a test for possible nonspecific effects of CntxMII on locomotion, we studied the effects of intra-VTA CntxMII on novelty-elicited locomotion. CntxMII (1 or 10 μM) or aCSF were bilaterally perfused into the VTA for 15 min through microdialysis probes as described above, starting 15 min before placing the rat in an activity cage. Novelty-elicited locomotion was measured during the following 60 min. No significant difference between CntxMII (1 μM, $n = 6$; 10 μM, $n = 5$) and aCSF ($n = 14$) intra-

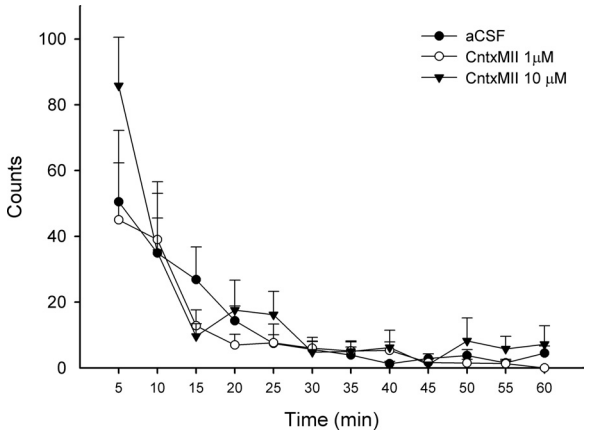

Figure 9. Effects of intra-VTA perfusion (15 min before rat placement into the activity cage) of CntxMII (1 or 10 μM) on novelty-elicited locomotion. Error bars indicate SEM. Statistical analysis was according to repeated-measures ANOVA. No significant group effect was detected. Group size: aCSF, 14 rats; CntxMII (1 μM), 6 rats; CntxMII (10 μM), 5 rats.

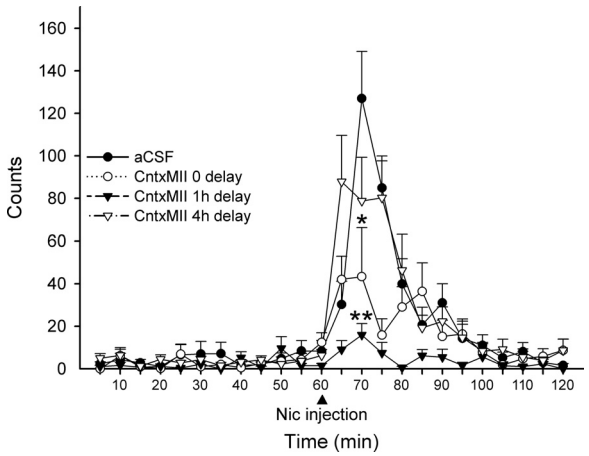

Figure 10. Effects of 10 μM CntxMII perfused for 15 min into the VTA on habituated locomotion elicited by nicotine (0.4 mg/kg base, i.p.) injected immediately after, 1 or 4 h after the end of CntxMII perfusion. Mean values are shown. Error bars indicate SEM. Statistical analysis was according to repeated-measures ANOVA; $^*p < 0.05$, $^{**}p < 0.01$ versus Nic+aCSF. Group size: aCSF, 11 rats; 0 delay, 6 rats; 1 h delay, 7 rats; 4 h delay, 10 rats.

VTA perfusion was detected (repeated-measures ANOVA, time: $F_{(5,22)} = 13.38$, $p < 0.001$; groups: $F_{(2,22)} = 0.30$, $p = 0.741$; time by groups: $F_{(10,22)} = 0.98$, $p = 0.462$) (Fig. 9).

Effects of different delays between intra-VTA CntxMII perfusion and systemic nicotine administration

As described above, 10 μM CntxMII perfused into the VTA through bilateral cannulae was able to markedly but not completely inhibit nicotine stimulating action on habituated locomotion. A possible explanation for this partial effect is that CntxMII did not have sufficient time to diffuse into the VTA and reach all the relevant molecular targets. We, therefore, tested several delays, 0, 1, or 4 h, between 15 min CntxMII (10 μM) perfusion and nicotine intraperitoneal injection. As shown in Figure 10, rats challenged with systemic nicotine immediately after or 1 h after intra-VTA CntxMII perfusion showed a partial or complete block of nicotine-elicited habituated locomotion, respectively. Instead, a 4 h delay led to an almost complete recovery of nicotine effect [repeated-measures one-way ANOVA, $F_{(3,30)} = 9.91$, $p < 0.001$; Dunnett's *post hoc* test vs Nic+aCSF: Nic+CntxMII (0 delay), $p = 0.043$; Nic+CntxMII (1 h delay), $p < 0.001$; Nic+CntxMII (4 h delay), NS].

Effects of intra-VTA perfusion of CntxMII on intravenous nicotine self-administration

Stable responding for nicotine self-administration was reached after 19.4 ± 4.3 nicotine self-administration sessions (means ± SD). At stability, the average number of nicotine infusions/session was 19.0 ± 1.0, with an average nicotine intake of 0.5 ± 0.1 $mg \cdot kg^{-1} \cdot session^{-1}$. Rate of responding was 111.0 ± 8.5 and 9.1 ± 1.7 active and inactive lever presses, respectively (means ± SEM of the last three self-administration sessions before starting the testing phase; data only from rats with correct VTA guide cannulae placements, $n = 13$).

On test sessions, CntxMII (10 μM) or aCSF were perfused for 15 min and rate of responding was recorded for the following hour. Note that previous experiments (see above, Effects of different delays between intra-VTA CntxMII perfusion and systemic nicotine administration) showed that CntxMII could effectively inhibit nicotine-elicited locomotion for at least 1 h after 15 min perfusion. CntxMII (10 μM) perfused into the VTA through bilateral guide cannulae was able to markedly reduce responding for nicotine self-administration (9.9 ± 1.8 number of nicotine infusions/session) compared with baseline sessions (18.4 ± 1.4 mean number of nicotine infusions/session of the last three self-administration sessions; means ± SEM) (Fig. 11*A*). Rate of responding decreased from 104.4 ± 10.8 (baseline sessions) to 52.8 ± 12.4 (CntxMII test session) mean ± SEM active lever presses/session (Fig. 11*B*). The observed decrease (~50%) in nicotine self-administration induced by intra-VTA perfusion of CntxMII is comparable with that observed in the same paradigm after the administration of other nicotinic antagonists, such as mecamylamine and dihydro-β-erythroidine (for review, see Lerman et al., 2007).

The statistical analysis performed by means of paired sample Student's *t* test on test session values − baseline session values showed that intra-VTA 10 μM CntxMII pretreatment significantly decreased the number of nicotine infusions/session with respect to aCSF pretreatment ($t = 2.84$; $p = 0.016$; df = 11).

No significant changes were observed for inactive lever presses after CntxMII pretreatment (paired sample Student's *t* test, $t = 1.69$; $p = 0.122$; df = 10) (Fig. 11*B*). A high number of inactive lever presses during aCSF test session (179 presses/1 h) was observed for subject CO2. Considering that the same subject did not show significant changes during CntxMII session compared with baseline (9.0 vs 5.7 inactive lever presses/1 h) and that the group average for CntxMII test day was not significantly different from baseline values, nonspecific effects of CntxMII perfusion on inactive lever presses could be excluded.

Using the same bilateral perfusion protocol, no significant effect of intra-VTA CntxMII (10 μM) was observed on food-maintained responding (Fig. 12). On test sessions, CntxMII or aCSF were perfused for 15 min and rate of responding was recorded for the following hour. The 10 μM CntxMII perfusion into the VTA was not able to significantly reduce responding for food (45.3 ± 7.6 number of food reinforcers/CntxMII test session vs 54.5 ± 1.2 mean number of food reinforcers/session of the last three baseline sessions) compared with aCSF perfusion (50.5 ± 3.3, number of food reinforcers/aCSF test session, vs 55.1 ± 0.9, mean number of food reinforcers/session of the last three baseline sessions; paired sample Student's *t* test on test − baseline values, $t = 0.586$, $p = 0.583$, df = 5).

In addition, CntxMII pretreatment was not able to alter the number of either active or inactive lever presses with respect to aCSF

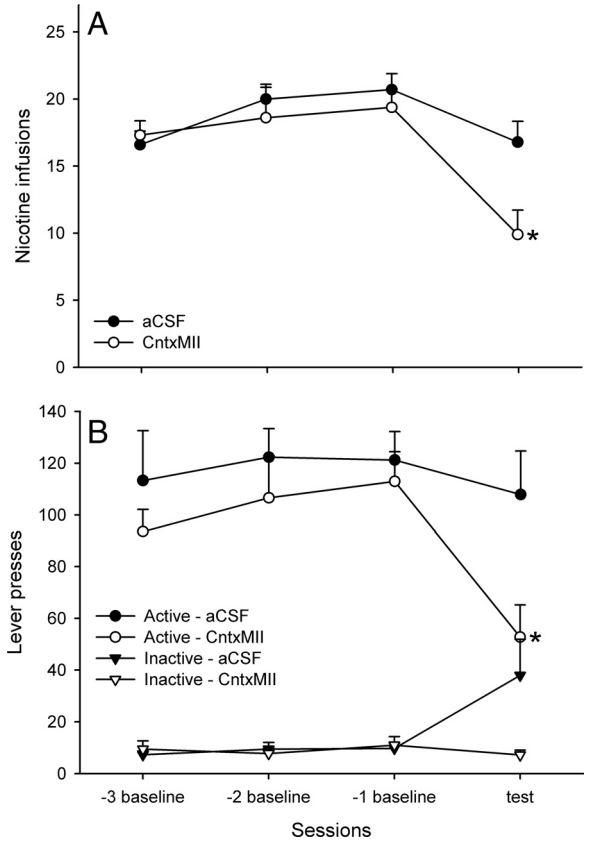

Figure 11. Effects of CntxMII on responding in rats trained to self-administer nicotine. CntxMII (10 μM) or aCSF were perfused into the VTA for 15 min before the start of the test session. ***A***, Number of nicotine infusions. The marks represent the number of infusions/1 h session during the three last sessions (baseline) before the CntxMII (open circles) or aCSF (filled circles) test sessions. ***B***, Number of active and inactive lever presses. The marks represent the number of active (circles) or inactive (triangles) lever presses/1 h session during the three last sessions (baseline) before the CntxMII (open symbols) or aCSF (filled symbols) test sessions. CntxMII (10 μM) or aCSF were perfused for 15 min before the start of the test session. The statistical analysis was performed by means of paired sample Student's *t* test on test session values − baseline session values; $*p < 0.05$. Mean ± SEM values are shown. $n = 12$ rats/group.

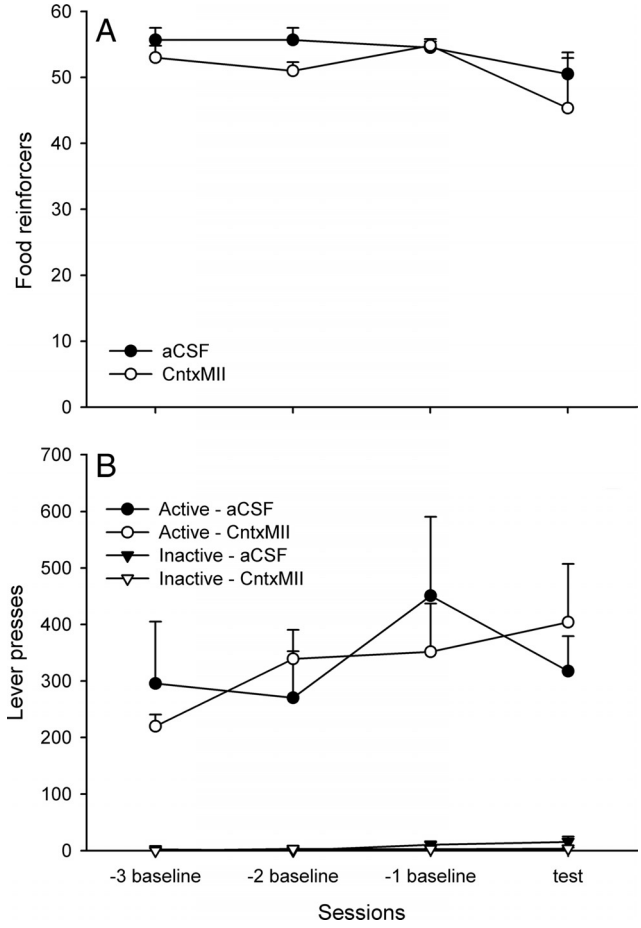

Figure 12. Effects of CntxMII on food-maintained responding in rats. ***A***, Number of food reinforcers. The marks represent the number of reinforcers/1 h session during the three last sessions (baseline) before the CntxMII (open circles) or aCSF (filled circles) test sessions. ***B***, Number of active and inactive lever presses. The marks represent the number of active (circles) or inactive (triangles) lever presses/1 h session during the three last sessions (baseline) before the CntxMII (open symbols) or aCSF (filled symbols) test sessions. CntxMII (10 μM) or aCSF were perfused for 15 min before the start of the test session. The statistical analysis was performed by means of paired sample Student's *t* test on test session values − baseline session values. No significant group effect was detected. Mean ± SEM values are shown. $n = 6$ rats/group.

pretreatment (active lever presses; CntxMII: 404.2 ± 103.0/test vs 316 ± 59.7/baseline; aCSF: 317.5 ± 62.0/test vs 377.1 ± 79.6/baseline; paired sample Student's *t* test, $t = -1.75$, $p = 0.141$, df = 5; inactive lever presses; CntxMII: 6.1 ± 3.1/test vs 5.1 ± 2.9/baseline; aCSF: 14.4 ± 8.6/test vs 7.8 ± 3.2/baseline; paired sample Student's *t* test, $t = -0.87$, $p = 0.425$, df = 5) (Fig. 12).

The results of this experiment support the specificity of CntxMII effects on nicotine self-administration and indicate that the intra-VTA bilateral perfusion of CntxMII at the 10 μM dose does not cause nonspecific changes in lever pressing.

Discussion

α6β2* nAChRs expressed in midbrain DA neurons are heterogeneous

Present immunochemical analysis shows a partial regional heterogeneity of nAChR subtypes in mesostriatal DA neurons. Whereas α6* receptors expressed by nigrostriatal DA terminals are almost exclusively α4α6β2β3 receptors, the majority of α6* receptors expressed by mesolimbic terminals are α6β2β3 receptors. In addition, a minor population of α4β2β3 receptors is expressed in the CPu. The much higher prevalence of receptors with two α6β2 binding interfaces in ventral striatum may contribute to explain the different sensitivity to systemic nicotine of nigrostriatal and mesolimbic pathways (Di Chiara and Imperato, 1988; Janhunen and Ahtee, 2007). Purely α6 or mixed α4α6 receptors may have different pharmacological and physiological, and perhaps also cell biology, properties. The mixed α4α6β2 receptor has higher affinity for nicotinic agonists than the α6β2 receptor (Salminen et al., 2007), and chronic nicotine (Perez et al., 2008) has opposite effects on the expression of these subtypes in the striatum. These findings may possibly explain the recent evidence of a dominance of purely α6*-sensitive responses in the nAc, whereas α4 responses dominate in the CPu (Exley et al., 2008).

A second heterogeneity concerns nerve terminal versus cell body/dendrite compartments of DA neurons. Although the present study could not discriminate the substantia nigra from the VTA and may therefore hide additional heterogeneities, the present findings show that the cell body/dendrite compartment contains peculiar nAChR subtypes. In fact, no receptors with double α6β2 interfaces seem to exist in the ventral midbrain DA neurons, whereas putative α2β2* receptors could be detected only in DA neurons of this region. Although the low absolute

amount of Epi binding immunoprecipitated by α2 antibody prompts some caution on this latter result, it should be noticed that a previous paper showed that α2 mRNA is expressed by midbrain DA neurons (Charpantier et al., 1998).

Differently from striatum, in ventral midbrain we obtained evidence of α6β3β2* nAChR expression in non-DA neurons, presumably ganglionic terminals in the MT. Instead, we did not obtain evidence for α6* nAChR expression in a subpopulation of GABA neurons, previously described in the substantia nigra pars reticulata with electrophysiology coupled to single-cell PCR approach (Klink et al., 2001), perhaps because of its very low concentration. Finally, non-DA neurons of ventral midbrain express substantial levels of α3, β4, and β3 subunits, which should belong to α3β3β4* receptors expressed by the fibers of the fasciculus retroflexus, which, in addition, express α3β2(non-β4)* nAChRs (Whiteaker et al., 2002; Grady et al., 2009).

Overall, the present and previous results demonstrate that, in the ventral midbrain, most α6β3β2* nAChRs are expressed by DA cell bodies and/or dendrites, with a substantial minority of this subtype expressed by retinal afferents in MT. α3β3β4* and, to a more limited extent, α3β2* nAChRs are expressed by axons/terminals of the habenulo-interpeduncular pathway. More discriminative approaches, such as optic and electron microscopy, are required to complete the complex picture of nAChR subtypes in this region.

Intracerebrally perfused CntxMII and CntxPIA bind α6β2*/α3β2* and α6β2* nAChRs, respectively

A main issue has been to evaluate the effective concentration of conotoxins perfused into the brain and therefore their selectivity for nAChR subtypes. The experiment on ^{125}I-CntxMII perfusion shows that ~5% of the toxin can cross the dialysis membrane in present experimental conditions. This figure is slightly lower than that of small molecules (10–15%) (Tang et al., 2003). An exponential decrease of the toxin concentration takes place diffusing into the tissue, so that the concentration at a distance of 1 mm from the membrane becomes 1% or less. The studies on protein binding of CntxMII in the brain show that <10% of the toxin is free and therefore available for binding to nAChRs. CntxMII and CntxPIA antagonize nicotine effects at a concentration of 1 and 10 μM in the perfusion liquid, respectively. We can reasonably calculate that the effective intratissue concentration of CntxMII and CntxPIA is between 5 and 1 nM and 50 and 10 nM, respectively, within 1 mm far from the dialysis cannula. According to the literature and present binding data, these concentrations are selective for α6β2 binding interfaces. In self-administration experiments, CntxMII was perfused at 10 μM concentration and may partially block α3β2* nAChRs, too.

α6β2* nAChRs expressed in the VTA are necessary for systemic nicotine effects on DA release, habituated locomotion, and reinforcement

The main result of this study is that CntxMII and CntxPIA perfused into the VTA inhibit nicotine-elicited DA release in nAc and habituated locomotion. In addition, intra-VTA CntxMII pretreatment significantly reduces responding for nicotine self-administration at an extent comparable with that previously obtained with other nicotinic antagonists in the same paradigm. This latter finding has been obtained with a valid rat model of nicotine reinforcement behavior, under experimental and nicotine dosing conditions widely used for studying the reinforcing effects of nicotine (Vezina et al., 2007; Markou et al., 2008). Although preliminary, these data strongly suggest that VTA CntxMII-sensitive receptors contribute to the activation of DA mesolimbic pathway elicited by intravenously self-administered nicotine.

Recently, Pons et al. (2008) reported that α6 knock-out mice do not acquire acute intravenous nicotine self-administration, a model of initiation of nicotine self-administration. Overall, present and previous data on nicotine self-administration obtained with different protocols (acute or chronic) in different species (mice or rats) strongly support a major involvement of VTA α6* nAChRs in nicotine-reinforcing properties.

Present and previous data point to the fact that CntxMII/CntxPIA-sensitive receptors in the VTA consist of α6β2* nAChRs, expressed by midbrain DA neurons (see above). In addition, α3β2* nAChRs of the habenulo-interpeduncular system may in part contribute to inhibition of nicotine self-administration, as suggested by the implication of this pathway in reward processes (Glick et al., 2006; Taraschenko et al., 2007; Morissette and Boye, 2008). Note, however, that available evidence points to a relevant role of α3β4* rather than α3β2* nAChRs. Therefore, the present findings strongly support the notion that α6β2* nAChRs expressed by DA neurons of the VTA are necessary for DA release in nAc, locomotion, and reinforcement elicited by systemic nicotine administration.

A functional role of α6β2* nAChRs expressed by DA mesostriatal neurons has been repeatedly demonstrated in *ex vivo* preparations in both striatum and midbrain (Klink et al., 2001; Champtiaux et al., 2003; Salminen et al., 2004, 2007; Drenan et al., 2008; Exley et al., 2008; Meyer et al., 2008). However, previous *in vivo* evidence for a physiological or pharmacological role of these receptors was in part contradictory. In accordance with present findings, intra-VTA infusion of anti-α6 oligonucleotides partially inhibits nicotine-elicited habituated locomotion in rats (Le Novère et al., 1999), and mice expressing gain-of-function α6* nAChRs show spontaneous hyperlocomotion that is exaggerated by low dose of systemic nicotine (Drenan et al., 2008). Instead, no significant change in systemic nicotine-elicited DA release in nAc was detected in α6$^{-/-}$ mice (Champtiaux et al., 2003). Note, however, that the increased concentration of α4β2* nAChRs detected in mesostriatal regions of α6$^{-/-}$ mice may compensate for the lack of α6β2* nAChRs (Champtiaux et al., 2003).

The present results show that VTA α6β2* receptors are necessary for some DA neuron-related effects of nicotine, but do not exclude the contribution of (non-α6)β2* receptors or α7 receptors (Schilström et al., 2000; Laviolette and van der Kooy, 2003; Mameli-Engvall et al., 2006). As regards β2* nAChRs, whose fundamental role in mediating nicotine effects on DA neurons and nicotine reinforcement has been clearly established (Picciotto et al., 1998; Maskos et al., 2005; Walters et al., 2006), a strong case has been made for α4β2* nAChRs. Available evidence shows that systemic nicotine-elicited DA release and acute self-administration are absent if α4* receptors are deleted (Marubio et al., 2003; Pons et al., 2008). An important role of α4* nAChRs is also suggested by the evidence that activation of hypersensitive α4* nAChRs is sufficient to support nicotine place preference (Tapper et al., 2004). Yet, at the moment, the pharmacological evidence of the contribution of α4β2* receptors to maintenance of nicotine self-administration is not conclusive, since the selectivity for α4β2* with respect to α6β2* nAChRs of available nicotinic antagonists or partial agonists (dihydro-β-erythroidine, SSR591813 [(5*aS*,8*S*,10*aR*)-5*a*,6,9,10-tetrahydro,7*H*,11*H*-8,10*a*-methanopyrido[2′,3′:5,6]pyrano[2,3-*d*]azepine], varenicline, UCI-30002 [*N*-(1,2,3,4-tetrahydro-1-naphthyl)-4-nitroaniline]) (Corrigall et al., 1994; Cohen et al., 2003; Rollema et

al., 2007; Yoshimura et al., 2007) is not well established. We propose that both α6β2 and α4β2 receptors are necessary for (at least some of) the effects of nicotine on the DA system. Therefore, blockade of either one or the other nAChR subtype strongly reduces or suppresses nicotine effects on the DA system.

Overall, the present experiments show that α6β2* nAChRs expressed in the VTA are necessary for the effects of systemic nicotine on DA release in the nAc, a main neurochemical target of addictive drugs (Di Chiara, 2000; Wise, 2002), and nicotine self-administration, a valid animal model of nicotine-reinforcing properties. Since these receptors are expressed almost exclusively in this brain region, α6β2*-selective compounds able to cross the blood–brain barrier would be promising drugs to affect nicotine addictive properties and, therefore, for the therapy of tobacco dependence with higher selectivity for the DA system and potentially fewer side effects than α4β2*-selective or subtype-nonselective compounds.

References

Azam L, Winzer-Serhan UH, Chen Y, Leslie FM (2002) Expression of neuronal nicotinic acetylcholine receptor subunit mRNAs within midbrain dopamine neurons. J Comp Neurol 444:260–274.

Blanchfield JT, Gallagher OP, Cros C, Lewis RJ, Alewood PF, Toth I (2007) Oral absorption and in vivo biodistribution of alpha-conotoxin MII and a lipidic analogue. Biochem Biophys Res Commun 361:97–102.

Brunzell DH, Boschen KE, Hendrick ES, Beardsley PM, McIntosh JM (2010) Alpha-conotoxin MII-sensitive nicotinic acetylcholine receptors in the nucleus accumbens shell regulate progressive ratio responding maintained by nicotine. Neuropsychopharmacology 35:665–673.

Champtiaux N, Gotti C, Cordero-Erausquin M, David DJ, Przybylski C, Léna C, Clementi F, Moretti M, Rossi FM, Le Novère N, McIntosh JM, Gardier AM, Changeux JP (2003) Subunit composition of functional nicotinic receptors in dopaminergic neurons investigated with knock-out mice. J Neurosci 23:7820–7829.

Charpantier E, Barnéoud P, Moser P, Besnard F, Sgard F (1998) Nicotinic acetylcholine subunit mRNA expression in dopaminergic neurons of the rat substantia nigra and ventral tegmental area. Neuroreport 9:3097–3101.

Cheetham SC, Viggers JA, Butler SA, Prow MR, Heal DJ (1996) [^{3}H]Nisoxetine—a radioligand for noradrenaline reuptake sites: correlation with inhibition of [^{3}H]noradrenaline uptake and effect of DSP-4 lesioning and antidepressant treatments. Neuropharmacology 35:63–70.

Chiamulera C, Tedesco V, Zangrandi L, Giuliano C, Fumagalli G (2010) Propranolol transiently inhibits reinstatement of nicotine-seeking behaviour in rats. J Psychopharmacol 24:389–395.

Cohen C, Bergis OE, Galli F, Lochead AW, Jegham S, Biton B, Leonardon J, Avenet P, Sgard F, Besnard F, Graham D, Coste A, Oblin A, Curet O, Voltz C, Gardes A, Caille D, Perrault G, George P, Soubrie P, et al. (2003) SSR591813, a novel selective and partial alpha4beta2 nicotinic receptor agonist with potential as an aid to smoking cessation. J Pharmacol Exp Ther 306:407–420.

Corrigall WA, Coen KM, Adamson KL (1994) Self-administered nicotine activates the mesolimbic dopamine system through the ventral tegmental area. Brain Res 653:278–284.

Corringer PJ, Le Novère N, Changeux JP (2000) Nicotinic receptors at the amino acid level. Annu Rev Pharmacol Toxicol 40:431–458.

Cox BC, Marritt AM, Perry DC, Kellar KJ (2008) Transport of multiple nicotinic acetylcholine receptors in the rat optic nerve: high densities of receptors containing alpha6 and beta3 subunits. J Neurochem 105:1924–1938.

Di Chiara G (2000) Role of dopamine in the behavioural actions of nicotine related to addiction. Eur J Pharmacol 393:295–314.

Di Chiara G, Imperato A (1988) Drugs abused by humans preferentially increase synaptic dopamine concentrations in the mesolimbic system of freely moving rats. Proc Natl Acad Sci U S A 85:5274–5278.

Dowell C, Olivera BM, Garrett JE, Staheli ST, Watkins M, Kuryatov A, Yoshikami D, Lindstrom JM, McIntosh JM (2003) α-Conotoxin PIA is selective for α6 subunit-containing nicotinic acetylcholine receptors. J Neurosci 23:8445–8452.

Drenan RM, Grady SR, Whiteaker P, McClure-Begley T, McKinney S, Miwa JM, Bupp S, Heintz N, McIntosh JM, Bencherif M, Marks MJ, Lester HA (2008) In vivo activation of midbrain dopamine neurons via sensitized, high-affinity alpha 6 nicotinic acetylcholine receptors. Neuron 60:123–136.

Exley R, Clements MA, Hartung H, McIntosh JM, Cragg SJ (2008) Alpha6-containing nicotinic acetylcholine receptors dominate the nicotine control of dopamine neurotransmission in nucleus accumbens. Neuropsychopharmacology 33:2158–2166.

Ferrari R, Le Novère N, Picciotto MR, Changeux JP, Zoli M (2002) Acute and long-term changes in mesolimbic dopamine pathway after systemic or local single nicotine injections. Eur J Neurosci 15:1810–1818.

Glick SD, Ramirez RL, Livi JM, Maisonneuve IM (2006) 18-Methoxycoronaridine acts in the medial habenula and/or interpeduncular nucleus to decrease morphine self-administration in rats. Eur J Pharmacol 537:94–98.

Gotti C, Moretti M, Clementi F, Riganti L, McIntosh JM, Collins AC, Marks MJ, Whiteaker P (2005a) Expression of nigrostriatal alpha 6-containing nicotinic acetylcholine receptors is selectively reduced, but not eliminated, by beta 3 subunit gene deletion. Mol Pharmacol 67:2007–2015.

Gotti C, Moretti M, Zanardi A, Gaimarri A, Champtiaux N, Changeux JP, Whiteaker P, Marks MJ, Clementi F, Zoli M (2005b) Heterogeneity and selective targeting of neuronal nicotinic acetylcholine receptor (nAChR) subtypes expressed on retinal afferents of the superior colliculus and lateral geniculate nucleus: identification of a new native nAChR subtype alpha3beta2(alpha5 or beta3) enriched in retinocollicular afferents. Mol Pharmacol 68:1162–1171.

Gotti C, Zoli M, Clementi F (2006) Brain nicotinic acetylcholine receptors: native subtypes and their relevance. Trends Pharmacol Sci 27:482–491.

Gotti C, Clementi F, Fornari A, Gaimarri A, Guiducci S, Manfredi I, Moretti M, Pedrazzi P, Pucci L, Zoli M (2009) Structural and functional diversity of native brain neuronal nicotinic receptors. Biochem Pharmacol 78:703–711.

Grady SR, Salminen O, Laverty DC, Whiteaker P, McIntosh JM, Collins AC, Marks MJ (2007) The subtypes of nicotinic acetylcholine receptors on dopaminergic terminals of mouse striatum. Biochem Pharmacol 74:1235–1246.

Grady SR, Moretti M, Zoli M, Marks MJ, Zanardi A, Pucci L, Clementi F, Gotti C (2009) Rodent habenulo-interpeduncular pathway expresses a large variety of uncommon nAChR subtypes, but only the α3β4* and α3β3β4* subtypes mediate acetylcholine release. J Neurosci 29:2272–2282.

Janhunen S, Ahtee L (2007) Differential nicotinic regulation of the nigrostriatal and mesolimbic dopaminergic pathways: implications for drug development. Neurosci Biobehav Rev 31:287–314.

Kalvass JC, Maurer TS (2002) Influence of nonspecific brain and plasma binding on CNS exposure: implications for rational drug discovery. Biopharm Drug Dispos 23:327–338.

Klink R, de Kerchove d'Exaerde A, Zoli M, Changeux JP (2001) Molecular and physiological diversity of nicotinic acetylcholine receptors in the midbrain dopaminergic nuclei. J Neurosci 21:1452–1463.

Laviolette SR, van der Kooy D (2003) The motivational valence of nicotine in the rat ventral tegmental area is switched from rewarding to aversive following blockade of the alpha7-subunit-containing nicotinic acetylcholine receptor. Psychopharmacology (Berl) 166:306–313.

Le Novère N, Changeux JP (1995) Molecular evolution of the nicotinic acetylcholine receptor: an example of multigene family in excitable cells. J Mol Evol 40:155–172.

Le Novère N, Zoli M, Changeux JP (1996) Neuronal nicotinic receptor alpha 6 subunit mRNA is selectively concentrated in catecholaminergic nuclei of the rat brain. Eur J Neurosci 8:2428–2439.

Le Novère N, Zoli M, Léna C, Ferrari R, Picciotto MR, Merlo-Pich E, Changeux JP (1999) Involvement of alpha6 nicotinic receptor subunit in nicotine-elicited locomotion, demonstrated by in vivo antisense oligonucleotide infusion. Neuroreport 10:2497–2501.

Lerman C, LeSage MG, Perkins KA, O'Malley SS, Siegel SJ, Benowitz NL, Corrigall WA (2007) Translational research in medication development for nicotine dependence. Nat Rev Drug Discov 6:746–762.

Lund JS, Remington FL, Lund RD (1976) Differential central distribution of optic nerve components in the rat. Brain Res 116:83–100.

Mameli-Engvall M, Evrard A, Pons S, Maskos U, Svensson TH, Changeux JP, Faure P (2006) Hierarchical control of dopamine neuron-firing patterns by nicotinic receptors. Neuron 50:911–921.

Markou A, Chiamulera C, West R (2008) Contribution of animal models and preclinical human studies to medication development for nicotine dependence. In: Animal and translational models for CNS drug discovery,

Vol 3, Reward deficit disorders (McArthur R, Borsini F, eds), pp 181–221. London: Academic.

Marubio LM, Gardier AM, Durier S, David D, Klink R, Arroyo-Jimenez MM, McIntosh JM, Rossi F, Champtiaux N, Zoli M, Changeux JP (2003) Effects of nicotine in the dopaminergic system of mice lacking the alpha4 subunit of neuronal nicotinic acetylcholine receptors. Eur J Neurosci 17:1329–1337.

Maskos U, Molles BE, Pons S, Besson M, Guiard BP, Guilloux JP, Evrard A, Cazala P, Cormier A, Mameli-Engvall M, Dufour N, Cloëz-Tayarani I, Bemelmans AP, Mallet J, Gardier AM, David V, Faure P, Granon S, Changeux JP (2005) Nicotine reinforcement and cognition restored by targeted expression of nicotinic receptors. Nature 436:103–107.

McIntosh JM, Azam L, Staheli S, Dowell C, Lindstrom JM, Kuryatov A, Garrett JE, Marks MJ, Whiteaker P (2004) Analogs of alpha-conotoxin MII are selective for alpha6-containing nicotinic acetylcholine receptors. Mol Pharmacol 65:944–952.

Meyer EL, Yoshikami D, McIntosh JM (2008) The neuronal nicotinic acetylcholine receptors alpha4* and alpha6* differentially modulate dopamine release in mouse striatal slices. J Neurochem 105:1761–1769.

Moretti M, Vailati S, Zoli M, Lippi G, Riganti L, Longhi R, Viegi A, Clementi F, Gotti C (2004) Nicotinic acetylcholine receptor subtypes expression during rat retina development and their regulation by visual experience. Mol Pharmacol 66:85–96.

Morissette MC, Boye SM (2008) Electrolytic lesions of the habenula attenuate brain stimulation reward. Behav Brain Res 187:17–26.

Mugnaini M, Garzotti M, Sartori I, Pilla M, Repeto P, Heidbreder CA, Tessari M (2006) Selective down-regulation of [^{125}I]Y0-alpha-conotoxin MII binding in rat mesostriatal dopamine pathway following continuous infusion of nicotine. Neuroscience 137:565–572.

Munson PJ, Rodbard D (1980) Ligand: a versatile computerized approach for characterization of ligand-binding systems. Anal Biochem 107:220–239.

Nisell M, Nomikos GG, Svensson TH (1994) Systemic nicotine-induced dopamine release in the rat nucleus accumbens is regulated by nicotinic receptors in the ventral tegmental area. Synapse 16:36–44.

Paxinos G, Watson C (2007) The rat brain in stereotaxic coordinates. Amsterdam: Academic.

Perez XA, Bordia T, McIntosh JM, Grady SR, Quik M (2008) Long-term nicotine treatment differentially regulates striatal alpha6alpha4beta2* and alpha6(Nonalpha4)beta2* nAChR expression and function. Mol Pharmacol 74:844–853.

Picciotto MR, Zoli M, Rimondini R, Léna C, Marubio LM, Pich EM, Fuxe K, Changeux JP (1998) Acetylcholine receptors containing the beta2 subunit are involved in the reinforcing properties of nicotine. Nature 391:173–177.

Pons S, Fattore L, Cossu G, Tolu S, Porcu E, McIntosh JM, Changeux JP, Maskos U, Fratta W (2008) Crucial role of $\alpha 4$ and $\alpha 6$ nicotinic acetylcholine receptor subunits from ventral tegmental area in systemic nicotine self-administration. J Neurosci 28:12318–12327.

Rollema H, Chambers LK, Coe JW, Glowa J, Hurst RS, Lebel LA, Lu Y, Mansbach RS, Mather RJ, Rovetti CC, Sands SB, Schaeffer E, Schulz DW, Tingley FD 3rd, Williams KE (2007) Pharmacological profile of the alpha4beta2 nicotinic acetylcholine receptor partial agonist varenicline, an effective smoking cessation aid. Neuropharmacology 52:985–994.

Salminen O, Murphy KL, McIntosh JM, Drago J, Marks MJ, Collins AC, Grady SR (2004) Subunit composition and pharmacology of two classes of striatal presynaptic nicotinic acetylcholine receptors mediating dopamine release in mice. Mol Pharmacol 65:1526–1535.

Salminen O, Drapeau JA, McIntosh JM, Collins AC, Marks MJ, Grady SR (2007) Pharmacology of alpha-conotoxin MII-sensitive subtypes of nicotinic acetylcholine receptors isolated by breeding of null mutant mice. Mol Pharmacol 71:1563–1571.

Schilström B, Fagerquist MV, Zhang X, Hertel P, Panagis G, Nomikos GG, Svensson TH (2000) Putative role of presynaptic alpha7* nicotinic receptors in nicotine stimulated increases of extracellular levels of glutamate and aspartate in the ventral tegmental area. Synapse 38:375–383.

Tang A, Bungay PM, Gonzales RA (2003) Characterization of probe and tissue factors that influence interpretation of quantitative microdialysis experiments for dopamine. J Neurosci Methods 126:1–11.

Tapper AR, McKinney SL, Nashmi R, Schwarz J, Deshpande P, Labarca C, Whiteaker P, Marks MJ, Collins AC, Lester HA (2004) Nicotine activation of alpha4* receptors: sufficient for reward, tolerance, and sensitization. Science 306:1029–1032.

Taraschenko OD, Shulan JM, Maisonneuve IM, Glick SD (2007) 18-MC acts in the medial habenula and interpeduncular nucleus to attenuate dopamine sensitization to morphine in the nucleus accumbens. Synapse 61:547–560.

Vezina P, McGehee DS, Green WN (2007) Exposure to nicotine and sensitization of nicotine-induced behaviours. Prog Neuropsychopharmacol Biol Psychiatry 31:1625–1638.

Walters CL, Brown S, Changeux JP, Martin B, Damaj MI (2006) The beta2 but not alpha7 subunit of the nicotinic acetylcholine receptor is required for nicotine-conditioned place preference in mice. Psychopharmacology (Berl) 184:339–344.

Whiteaker P, Peterson CG, Xu W, McIntosh JM, Paylor R, Beaudet AL, Collins AC, Marks MJ (2002) Involvement of the $\alpha 3$ subunit in central nicotinic binding populations. J Neurosci 22:2522–2529.

Wise RA (2002) Brain reward circuitry: insights from unsensed incentives. Neuron 36:229–240.

Yoshimura RF, Hogenkamp DJ, Li WY, Tran MB, Belluzzi JD, Whittemore ER, Leslie FM, Gee KW (2007) Negative allosteric modulation of nicotinic acetylcholine receptors blocks nicotine self-administration in rats. J Pharmacol Exp Ther 323:907–915.

Zanetti L, Picciotto MR, Zoli M (2007) Differential effects of nicotinic antagonists perfused into the nucleus accumbens or the ventral tegmental area on cocaine-induced dopamine release in the nucleus accumbens of mice. Psychopharmacology (Berl) 190:189–199.

Zoli M, Moretti M, Zanardi A, McIntosh JM, Clementi F, Gotti C (2002) Identification of the nicotinic receptor subtypes expressed on dopaminergic terminals in the rat striatum. J Neurosci 22:8785–8789.